FINAL REPORT
DOE Grant No.
DE-FG07-00ID13893
Task 5

Tracing Geothermal Fluids

Principal Investigator: Michael C. Adams
(madams@egi.utah.edu)
Co-Principal Investigator: Greg Nash
(gnash@egi.utah.edu)
Energy & Geoscience Institute
at the University of Utah
Salt Lake City, Utah, 84108

March, 2004

Executive Summary

Geothermal water must be injected back into the reservoir after it has been used for power production. Injection is critical in maximizing the power production and the lifetime of the reservoir. To use injectate effectively the direction and velocity of the injected water must be known or inferred. This information can be obtained by using chemical tracers to track the subsurface flow paths of the injected fluid. Tracers are chemical compounds that are added to the water as it is injected into the reservoir. The hot production water is monitored for the presence of this tracer using the most sensitive analytic methods that are economically feasible. The amount and concentration pattern of the tracer revealed by this monitoring can be used to evaluate how effective the injection strategy is.

However, the tracers must have properties that suite the environment they will be used in. This requires careful consideration and testing of the tracer properties. In previous and parallel investigations we have developed tracers that are suitable for tracing liquid water. In this investigation, we developed tracers that can be used for steam and mixed water/steam environments. This work will improve the efficiency of injection management in geothermal fields, lowering the cost of energy production and increasing the power output of these systems.

Tracing Geothermal Fluids

Introduction

Before 1983, when our DOE-sponsored injection research began, few tracers were available to the industry (ADAMS, 1985). At that time, the only tracers that had been used in geothermal systems were the inorganic halide ions, either radioactive (MCCABE et al., 1983) or stable (HORNE et al., 1987), and two fluorescent dyes, fluorescein (GUDMUNDSSON et al., 1983) and rhodamine WT (GUDMUNDSSON et al., 1984). The stable halides suffer from high background concentrations in geothermal systems, which require that extremely large quantities be used for a tracer test. Although background concentrations of radioactive halides are quite low, their short half-lives and the public reaction to injecting a radioactive compound makes them unacceptable. The two dyes were believed to be useful, but nothing was known of their stability at reservoir temperatures prior to our work.

From 1983 to 1989, we focused on liquid tracers. During this time we performed research that defined the stability of fluorescein (ADAMS and DAVIS, 1991), rhodamine WT (ROSE and ADAMS, 1994), and many aromatic acids (ADAMS et al., 1992). We field-tested several of these tracers in the first multiple-tracer, multiple-well field test ever performed in the geothermal industry (ADAMS et al., 1989). In 1989 the operators at The Geysers asked DOE for research that would help them stem reservoir pressure decline and maintain production from this important resource. Tracers were specifically called out. Several chlorofluorocarbon (CFC) gas tracers were quickly developed (ADAMS et al., 1991b) and deployed at The Geysers (ADAMS et al., 1991a). From 1991 to 1997, several tests were performed with one of the gas tracers, R-13 (BEALL et al., 1994). When production of the CFC R-13 was cut back because of international agreements, two hydrofluorocarbons (HFCs), R-134a and R-23, were chosen to replace it (ADAMS, 1999; BEALL et al., 1998).

These compounds were still under development when this contract began. Therefore the first task under the new contract was to define the thermal stability using laboratory studies.

Development of some additional liquid dye tracers, the sulfonated naphthalenes, was also begun during this time (ROSE et al., 2001). Detection limits were reduced to the parts per trillion range by switching from a filter fluorometer to a fluorescence spectrometer, and selectivity was improved by developing liquid chromatographic methods. An analytic method using laser-induced fluorescence was then developed at EGI by Peter Rose, under a separate DOE grant, which lowered this detection limit to the parts per quadrillion range.

Our choice of tracers has generally been driven by the preferences of the U.S. geothermal industry. Operators of liquid-dominated systems prefer the more expensive fluorescent tracers because they can analyze them on-site, rather than using an inexpensive tracer that has to be sent out for analysis. Operators of vapor-phase systems, in contrast, are used to steam-sampling techniques being more expensive and are located near the analytic laboratories that analyze the vapor-phase tracers. They are willing to pay much more for analysis and much less for the compound itself. These preferences have driven the tracer development in very different directions for liquid- versus vapor-dominated systems.

Liquid- and vapor-phase tracers have some properties in common. All ideal tracers should be inexpensive, environmentally safe, non-adsorptive, detectable at low concentrations, and absent from natural waters. Thermal stability is also an important consideration. An ideal tracer should not decay at all if it is designed to simply track the flow of water. In practice, a tracer can decay if the decay rate can be defined and compensated for. In liquid systems, two tracers with known decay rates can be used simultaneously. As shown in ADAMS et al. (1989), the changing ratio of the two tracers can not only be used to calculate the pre-decay concentrations, but also to define a temperature parameter for the flow path. Liquid tracers should also be extremely soluble in liquid water, and the solubility should be accomplished by ionization of the compound as well as a high polarity. This prevents the liquid tracer from fractionating into the vapor (steam) phase. The lack of fractionation prevents the tracer from entering any steam zones along the injection-production flow path. Fractionating into a steam zone would remove the tracer from the liquid flow path, skewing the results of the tracer test. The lack of volatility also makes sampling much easier. Liquid sampling of geothermal water can be accomplished by simply turning a valve and running the water through a cooling coil into an open plastic bottle.

The vapor-phase tracers that we have developed fractionate strongly into the steam phase. This is necessary in order for the tracers to track the flow of steam through the reservoir. The increased volatility has several implications that make vapor-phase tracers more difficult to design and use. The primary effect results from the fact that although steam is produced from vapor-phase reservoirs, the water that is injected back into the ground is always liquid. Therefore, vapor-phase tracers, which are sparingly soluble as a consequence of their high volatility, are injected at low concentrations. When they reach boiling temperatures in the reservoir, they immediately travel into the steam phase with the first small fraction of steam created. Very little is left in the residual water to track it to its ultimate destination. The second effect of the volatility is that different compounds enter the steam phase at different rates. The rate for each compound depends on its solubility. Consequently, the decay rate of vapor-phase tracers cannot be used to define pre-decay concen-

trations or any temperature parameters of the flow path. This situation creates a solubility-dependent ratio in production steam of any two volatile tracers that were injected simultaneously. This effect has been detected in two tests conducted at The Geysers in which tritiated water was injected simultaneously with a vapor-phase tracer (Adams, 2001).

The second task under the new contract was to create models that would estimate the effects of volatility on the outcomes of tracer tests in vapor-dominated systems.

Because of their volatility, vapor-phase tracers do not always follow the same path as the injected water that does not immediately boil. For example, Adams (2001) has shown that wells in which the vapor-phase tracers appeared can have a different geographic distribution than those of the tritium tracer, even though the two types of tracers were simultaneously injected. Calculations of injectate recovery are also skewed when this situation occurs. This is an important consideration, one that will become increasingly relevant as the amount of injection increases due to the Lake and Sonoma County pipelines. In contrast, there is considerable evidence from other tracer tests at The Geysers that the path of the vapor-phase tracers and the bulk of the injection-derived steam coincide (Adams et al., 1991; Beall et al., 1994; Adams, 1999). This situation occurs when the liquid injectate boils completely within a short distance of the injection well.

Therefore, in some cases, a distribution coefficient similar to that of water may be desirable in order to more closely follow the behavior of the injected fluid. A tracer with significant solubility in water but which volatilizes at a rate near that of water can be termed a two-phase tracer (water and steam).

The third task of the new contract was to develop these two-phase tracers for use in geothermal systems.

Tracer tests produce an abundance of data that must be rapidly examined in order to control the sampling schedule, a prime method of controlling costs during tracer tests. The geographic distribution of the tracer returns and the time trends for each well in real time are the most useful tools in modifying the sampling schedule accordingly.

The fourth task was to create an interface with a conventional geographic information system (GIS) that will facilitate this interpretation.

Technology transfer is always an important facet of applied research. As the primary developers of geothermal tracers we have been asked to be Guest Editors of a special issue of Geothermics devoted to the topic of geothermal tracers.

The fifth task was to locate people doing cutting-edge research on geothermal tracers and convince them to contribute to the issue, and then edit the resultant volume for the journal Geothermics.

Summary of Objectives

The major objectives of the proposed investigation were to:

1) Complete the development of geothermal vapor-phase tracers;
2) Develop interpretation techniques to define the conditions that might produce vapor-phase tracer separation in the reservoir;
3) Identify and test a class of compounds with the desired properties of a two-phase tracer;
4) Develop a software package that will provide a GIS interface for tracer test interpretation; and
5) Facilitate a special issue of the journal Geothermics dedicated to the topic of geothermal tracers.

Results

Task 1 – Finish stability studies of the new vapor-phase tracers

Vapor-phase tracers are useful in nearly all types of geothermal systems. They have been used in liquid-dominated (UPSTILL-GODDARD and WILKINS, 1995), two-phase (BIXLEY et al., 1995; MOORE et al., 2000), and vapor-dominated fields (ADAMS et al., 1991a; BEALL et al., 1994; BEALL et al., 1998). Vapor-phase tracers are of particular and immediate importance at The Geysers because vapor-dominated systems are water-poor and injection is a component vital to the longevity of the field. Artificial and natural tracers have been used at The Geysers to identify and track the flow of injected water and to evaluate the recovery of injectate. However, the natural tracers have become ineffective as the surface facilities were adapted to conserve steam for reinjection, and the most successful artificial tracers, chlorofluorocarbons, were taken off the market because of their deleterious effect on ozone concentrations in the upper atmosphere. R-134a and R-23, both hydrofluorocarbons, were proposed in 1997 as substitute geothermal tracers for the chlorofluorocarbons (ADAMS, 1997).

R-134a is a replacement for some of the chlorofluorocarbons previously used in refrigeration, air conditioning, foam blowing, pharmaceutical inhalers, and fire suppressants. Like the chlorofluorocarbons, many of the hydrofluorocarbons are inflammable, non-toxic, and relatively inert. The toxicity of hydrofluorocarbons is generally even lower than that of corresponding brominated and chlorinated hydrocarbons because of the higher stability of the carbon-fluorine bond. R-134a has very low acute and subchronic inhalation toxicity, has no chronic toxicity, and is nei-

ther a developmental toxicant nor genotoxic. Hydrofluorocarbons are, however, somewhat less stable at high temperatures than the chlorofluorocarbons. They are also less detectable using an electron capture detector, which was the preferred method for the chlorofluorocarbon tracers. However, an analytical method has been developed by Thermochem, Inc., which yields detection limits on the order of 10 to 100 parts per trillion. This method uses an enrichment procedure coupled with gas chromatography. A megabore porous polymer capillary column is used to separate the tracers from each other and from potentially interfering compounds. A modified Halogen-Specific Detector is used for detection.

Hydrofluorocarbons do not contribute to ozone depletion in the atmosphere because they do not contain chlorine or bromine atoms. Their vapor pressures are similar to their chlorofluorocarbon analogues, but they are considerably more soluble. A comprehensive list of hydrofluorocarbons and their properties can be found in ADAMS et al. (1991b).

Several successful field tests have now been performed using R-134a and R-23 (ADAMS, 1999; BEALL et al., 1998). During FY2000 we focused our laboratory tests on quantifying the thermal stability of R-134a in pure water. These tests are now complete and have been published (ADAMS et al., 2001; ADAMS and KILBOURN, 2000). The results are summarized in Table 1 and Figure 1.

Table 1. Summary of kinetic parameters derived from the R-134a experiments.

270°C: $k = 1.72 \times 10^{-7}$ s^{-1}
Coefficient of Determination, $r^2 = 0.92$
13 data points
290°C: $k = 4.97 \times 10^{-7}$ s^{-1}
Coefficient of Determination, $r^2 = 0.90$
15 data points
310°C: $k = 1.47 \times 10^{-6}$ s^{-1}
Coefficient of Determination, $r^2 = 0.90$
15 data points

E_a = 140,916 J/mol
ln (A) = 15.65 s^{-1}
Coefficient of Determination, r^2 = 0.999
3 data points

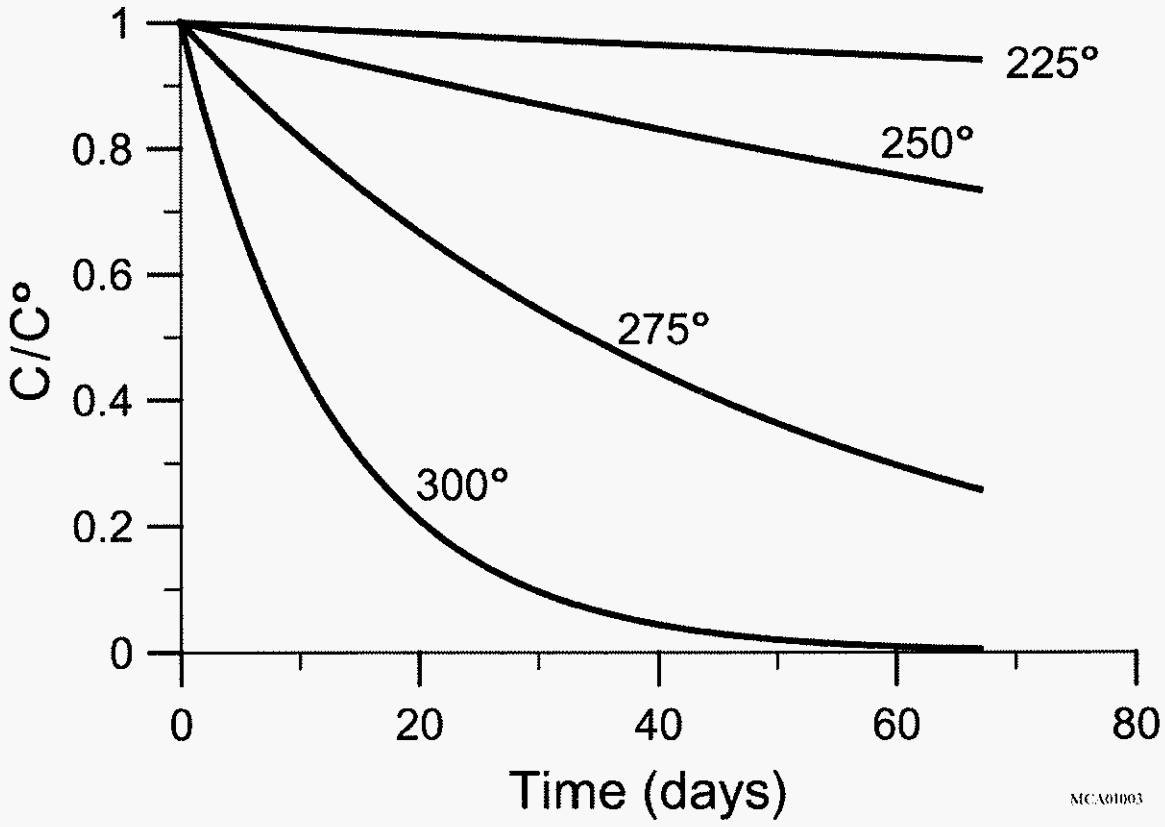

Figure 1. Time-decay plot for various temperatures. The plot was made using the kinetic parameters listed in Table 1.

Task 2 – Develop interpretation techniques to define the conditions that might produce vapor-phase tracer separation in the reservoir

Injection into a vapor-dominated system necessitates using a compound that can be dissolved in the liquid injectate but will fractionate to the steam phase once it is in the reservoir. Conventional tracers such as fluorescein or the naphthalene sulfonates cannot be used because they are ionic at reservoir pH's and will not fractionate to the steam phase. Thus, neutral species must be used as vapor-phase tracers. However, the volatility of these tracers can cause them to concentrate in the first small fraction of steam formed. This lowers the concentration of tracer

in the remaining liquid and any subsequently formed steam. If divergence of the liquid and steam flow occurred at fracture intersections during the early stages of boiling, the results of the tracer test could be skewed towards the direction of the steam-bearing fractures. The degree to which this occurs depends on the speed with which the steam leaves the liquid injectate and the distribution of fractures around the injection well.

The transfer of a volatile tracer to the steam phase can be calculated as a function of the steam fraction. The simplest method of doing this is to use a single-stage boiling model (HENLEY, 1984), which combines the mass balance shown in equation 1 with the liquid-vapor distribution coefficient (equation 2) to obtain the steam and liquid concentration as a function of the steam fraction (equations 3 and 4):

$$C_i^O = C_i^L(1-y) + C_i^V y \tag{1}$$

$$B_i = \frac{C_i^V}{C_i^L} \tag{2}$$

$$C_i^V = \frac{C_i^O}{\left(\frac{1-y}{B_i} + y\right)} \tag{3}$$

$$C_i^L = \frac{C_i^O}{(1 + y(B_i - 1))} \tag{4}$$

The first fraction of steam formed contains the highest concentration of tracer. In the single-stage model, it is assumed that all of the steam created by boiling will mix and equilibrate with the liquid as a mass with uniform concentration. This is the origin of the name, single-stage boiling. Instead of equilibrium partitioning in a "batch" mode, one can imagine a succession of boiling events in which equilibrated vapor is removed from contact with the liquid prior to the next boiling event. Because the tracer is more volatile than water, the tracer concentration in the first steam formed is highest, and successive boiling events would result in progressively lower concentrations of tracer. This is the basis of multiple-stage boiling models, in which "stages" of steam with a specified mass fraction are removed as they are formed. Concentrations of the tracer in the vapor and liquid are given by equations 5 and 6, respectively (HENLEY, 1984).

$$C_i^V = B_i C_i^O [1 + \Delta y(B_i - 1)]^{-n} \tag{5}$$

$$C_i^L = C_i^O [1 + \Delta y(B_i - 1)]^{-n} \tag{6}$$

Where n = the number of number of "boiling events", or "stages", in which a constant steam fraction Δy is evolved, equilibrated, and removed

from further contact with the liquid. There are two situations in which the multiple-stage model is pertinent. The first involves rapid movement of the steam away from the boiling liquid, so that it is not in contact with the liquid when it finally mixes with the later-formed steam. The second occurs when steam is removed in "batches" from the boiling liquid each time it passes through a fracture intersection.

The most rapid removal of tracer is obtained in situations similar to those that cause multiple-stage boiling, but in which the step size is infinitely small. The geologic analogue might be a liquid intersecting a steam-filled fracture in which the pressure gradient is extremely high. This is described by the continuous boiling model (DRUMMOND, 1981):

$$C_i^V = B_i C_i^O X^{(B_i-1)}, \text{and} \tag{7}$$

$$C_i^L = C_i^O X^{(B_i-1)}. \tag{8}$$

Where X = the fraction of initial liquid remaining, or 1-y.

Throughout this paper the boiling process will be discussed using the number of stages and the size of the steam fraction. The reader should keep in mind that these terms originate from modeling industrial processes, where equipment can be designed so that discrete boiling stages occur. Geologically, it is most likely that the variations in boiling conditions result from a continuum of fracture geometries and pressure gradients.

Equations 3 through 8 were used to simulate the effects of boiling during two tracer tests that were conducted at The Geysers. These two tests were chosen because two gas tracers and tritium were injected in each test, providing comparison of the hydrofluorocarbons, chlorofluorocarbons, and tritium as tracers. The first was conducted in 1994, in Unocal's DV-11 injection well (VOGE et al., 1994), and the second in 1998, in NCPA's P-1 injection well (ADAMS et al., 1999). The location of the tests is shown in Figure 2. These tests were cost-shared by DOE and industry in a program designed to evaluate the effects of increased injection on the pressure declines at The Geysers (ADAMS, 2001; VOGE et al., 1994).

The results of the simulations are shown in Figures 3-5. The first simulation in each figure is based on the concentrations and solubilities of the tracers used in the P-1 test, R-23 and R134a. The second is based on those used in the DV-11 test, SF_6 and R-13. The primary difference in the parameters of the two tests is that the more soluble hydrofluorocarbons were injected in nearly equal amounts in the P-1 test, while SF_6 and the chlorofluorocarbon R-13 were injected at a ratio of 1:1000 in the DV-11 test. In each figure the concentration of the tracers in both liquid and steam are plotted as a function of the steam fraction. The lowest concentration shown on the y-axis of each figure, $1x10^{-6}$ ppm, represents a nominal detection limit for SF_6 and the hydrofluorocarbons. The detec-

tion limit for R-13 was approximately $1x10^{-3}$ ppm. The actual detection limits depend on the gas content of the steam, and can vary by two orders of magnitude, although they more commonly vary within a factor of five. The liquid-vapor distribution coefficient of the tracers was held constant for these simulations, although it is in reality a function of temperature. The values used in the simulations were calculated using a temperature of 175°C, which is the approximate temperature of injectate boiling in this region of The Geysers due to depressurization related to exploitation.

The single-stage boiling simulations are shown in Figures 3a and 3b. These simulations display a linear trend on a log-log plot and a gentle decrease in the liquid and steam tracer concentrations with increasing steam fraction. The tracers would remain above the detection limits for the duration of the test under the conditions used in this simulation, providing a complete description of the distribution of the injectate as it boils. The changing ratio of the most soluble to the least soluble gas tracers during each test is shown at the top of Figures 3a and 3b. It can be seen that the ratio varies little during single-stage boiling. Slight enrichment of the least soluble tracer occurs at small steam fractions, although the ratio is identical to that in the injected liquid when the steam fraction exceeds 0.1.

The results of the multiple-stage boiling simulations show a significantly different picture. Figures 4a and 4b show that the tracer concentrations in both liquid and steam drop rapidly while the ratio of the two tracers in the steam increases to extremely high values. In these simulations a steam fraction (Δy) of 0.001 was arbitrarily chosen, and the number of stages (n) was set so that the cumulative steam fraction ranged from 0.001 to 0.9. Figures 5a and 5b show that the tracer concentrations in the continuous model decrease even more rapidly than in the multiple-stage model, reaching levels below detection at very low steam fractions.

The curves shown in Figures 3-5 can be transformed schematically to recovery curves, or tracer concentration versus time plots, as measured in the steam from the production wells. These are shown in Figure 6 for single-stage and multiple-stage boiling models using the R-134a parameters from the P-1 test. This figure was drawn by assuming that each arbitrary time unit was proportional to a steam fraction of 0.001, and that no dispersion occurred. The single-stage concentrations have one value because all of the steam equilibrated with the liquid as a single batch, and therefore Figure 6a does not mimic the curve shown in Figure 3a. The multiple-stage tracer concentrations (Fig. 6b) follow directly from Figure 4. The continuous boiling model is not plotted but is qualitatively similar to the multiple-stage model. The main differences between these two models are that the continuous boiling model would have higher

peak concentrations, and these maxima occur earlier than in the multiple-stage model.

It can be seen in Figure 6 that single-stage boiling produces a significantly different return curve than multiple-stage boiling. The concentrations are lower, and the duration of the response is prolonged. Multiple-stage boiling produce sharp peaks at much higher tracer concentrations, and shorter response durations. Although not shown in Figure 6, continuous boiling produces a curve similar to that from multiple-stage boiling, although with even higher peaks and shorter durations. These results suggest that conditions promoting single-stage boiling will reduce the effects of tracer volatility to the extent that the tracer will be measurable in the steam for larger boiling fractions, and for longer times. Multiple-stage boiling can exhaust the tracer from the injectate long before all of the injectate has boiled.

These results were compared with actual tracer tests at The Geysers using a variety of vapor-phase tracers. The comparison implies that the effects of volatility are exaggerated under conditions of high superheat, which promote the continuous removal of steam from the vicinity of the boiling interface. In contrast, low to moderate superheat reduces the effects of volatility to the extent that the volatile-tracer test results qualitatively resemble those in which tritiated water is used as a tracer. Thus, volatile tracers can be used with confidence to qualitatively describe the distribution of injected water in vapor-dominated systems where superheat is low to moderate. These conclusions are detailed in ADAMS (2001) and ADAMS et al. (2001).

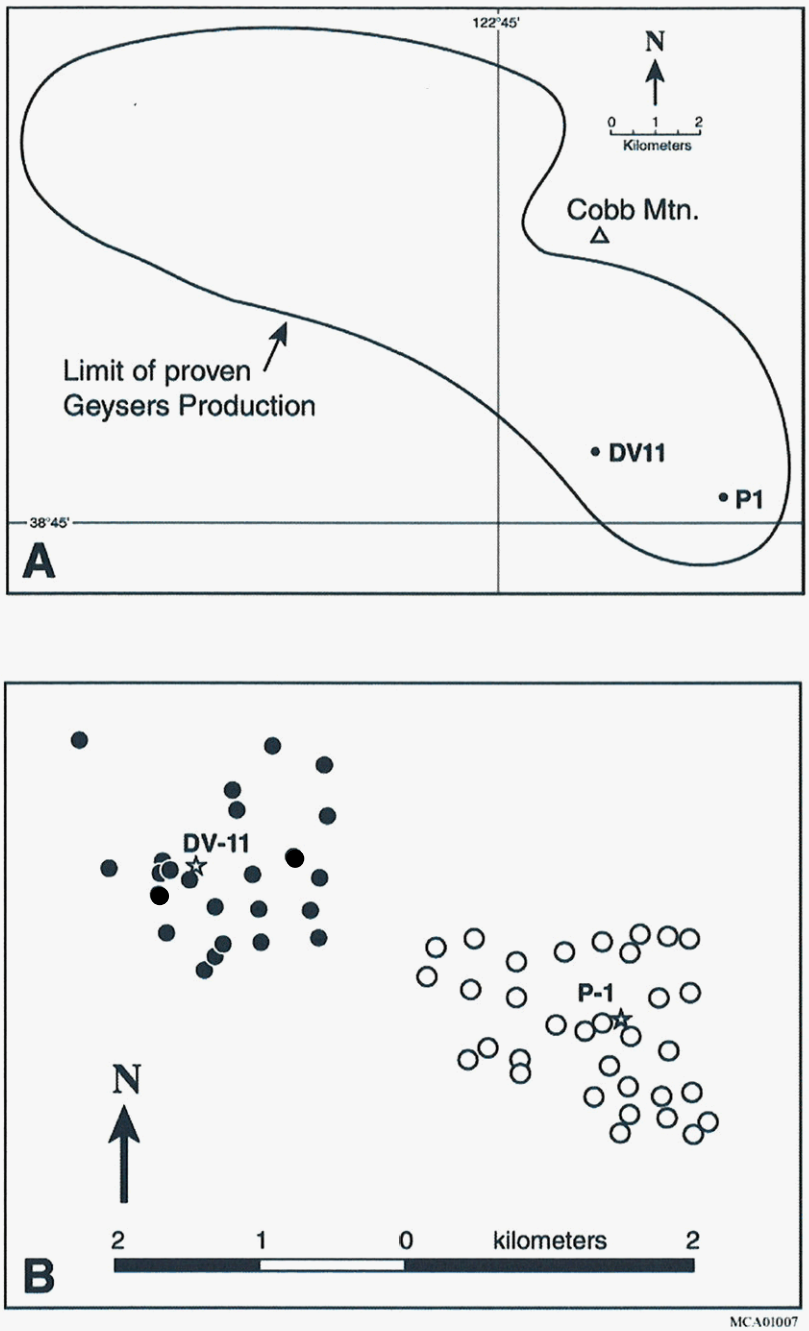

Figure 2. Location map of the DV-11 and P-1 tracer tests at The Geysers. The circles are the center-of-steam of the production wells and the stars show the location of the injection wells.

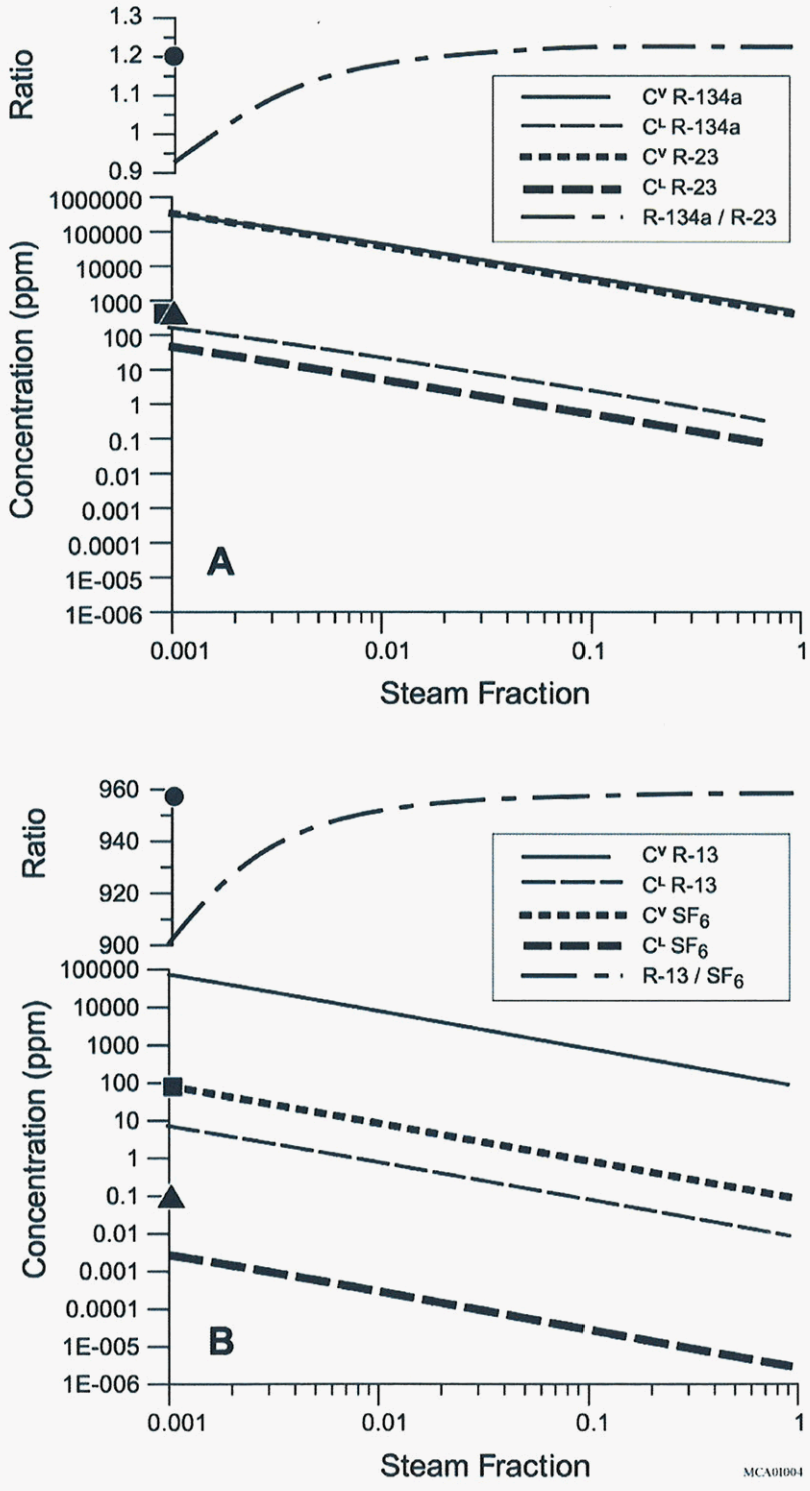

Figure 3. Single stage boiling. (a) Simulation of the P-1 test, in which R-134a (470 ppm) and R-23 (383 ppm) were injected as tracers. (b) Simulation of the DV-11 test, in which the less-soluble tracers SF_6 (0.085 ppm) and R-13 (81 ppm) were injected. The injection concentrations are shown by the symbols: circles = initial ratio, squares = R-134a or R-13, and triangles = R-23 or SF_6.

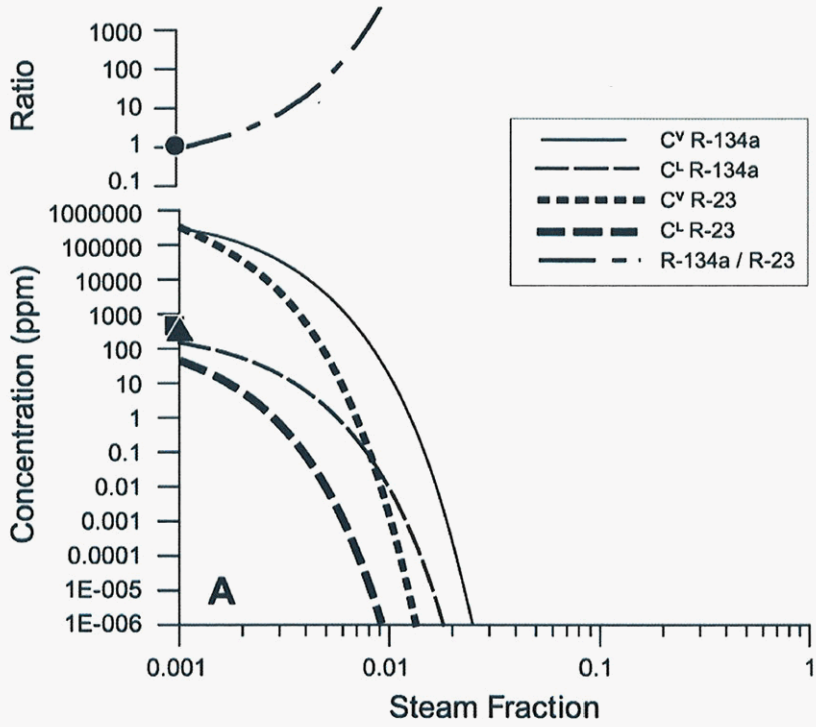

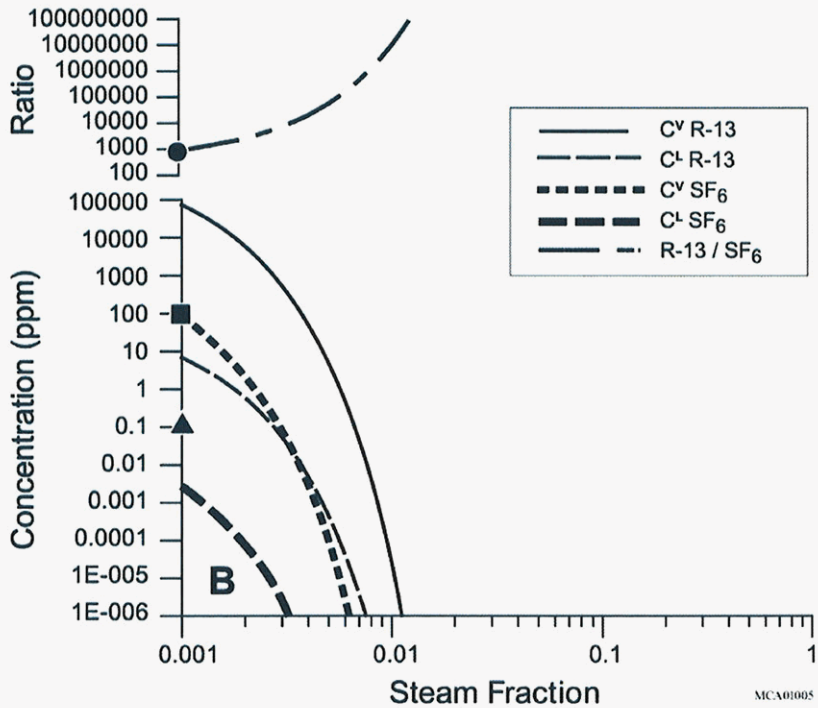

Figure 4. Multiple-stage boiling. This model represents steam generated from 30 stages of boiling (or 30 distinct fracture sets), with a steam fraction of 0.001 being generated at each fracture set. See Figure 3 for explanation.

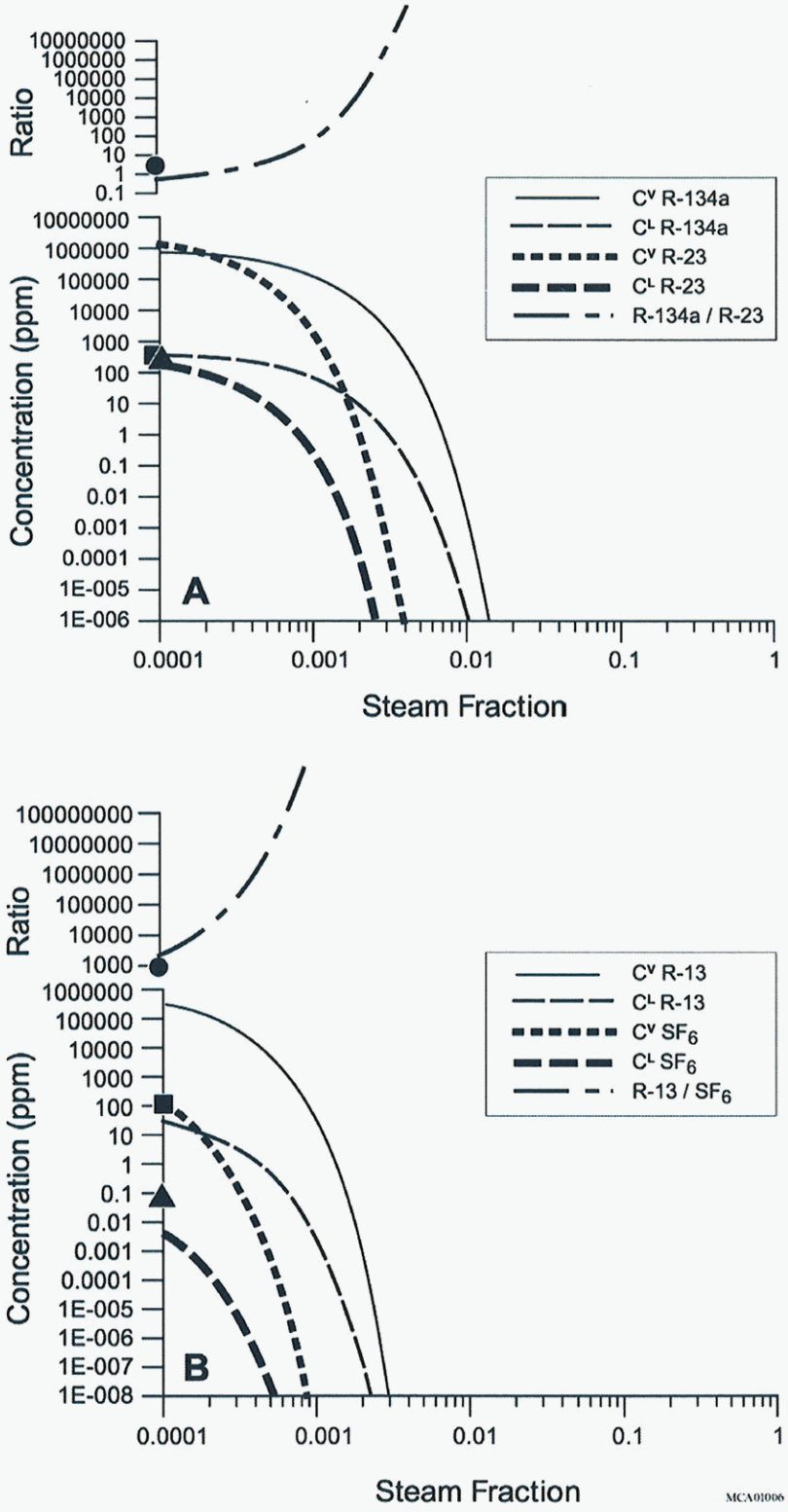

Figure 5. Continuous boiling. This model represents instantaneous removal of the steam from the liquid. See Figure 3 for explanation.

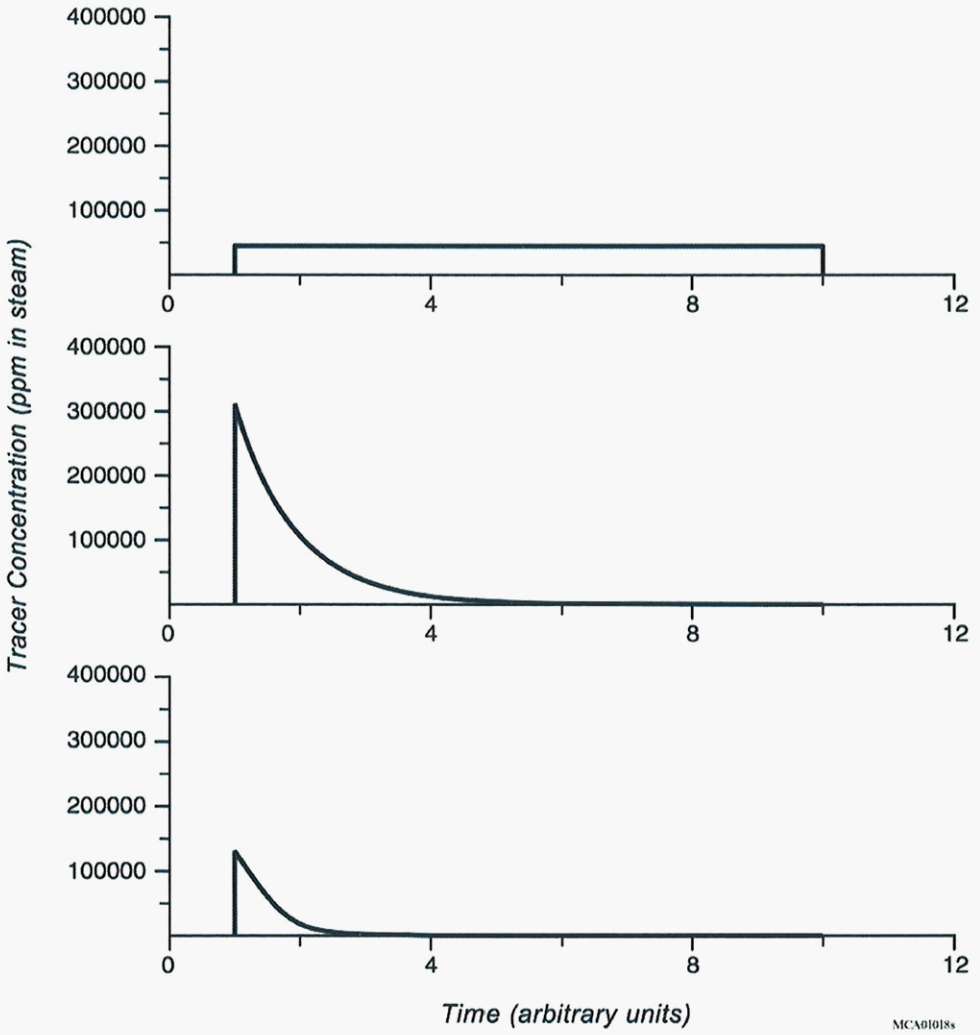

Figure 6. Schematic representation of the return curves that would result from the boiling simulations shown in Figures 3-5. The tracer concentrations shown are the steam concentrations of R-134a using the parameters of the P-1 test. The time units are equivalent to a steam fraction of 0.001. No processes that take place during transport, such as dispersion, are included in the transformation. (a) Single-stage boiling. (b) Multiple-stage boiling, and (c) Continuous boiling.

Task 3 – Identify and test a class of compounds with the desired properties of a two-phase tracer

Our initial work on two-phase tracers indicated that short-chain hydrocarbon alcohols might possess the properties we were looking for. They are very soluble in water, relatively nontoxic, polar but not ionized at geothermal temperatures and pH, and fairly stable at moderate to high temperatures.

Unfortunately, it was not feasible to use the hydrocarbon alcohols as tracers in the field at that time because they had a high detection limit on the available analytic equipment. We hypothesized that the addition of fluorine to the alcohols would provide a much lower detection limit using the detection techniques developed for the hydrofluorocarbons tracers in use at The Geysers. Those methods can be used to detect some fluorine-containing molecules at extremely low levels (ADAMS, 1999). Therefore, the next logical step in our research was to look at commercially available fluorinated alcohols.

All commercially available fluorinated compounds were considered so that no potential tracer was overlooked. Approximately 100 compounds were chosen from the thousands available. They were chosen on the basis of their elemental composition (C, O, H, and F), toxicity (low or irritant), size (<8 carbons), and acidity (pKa<10). A summary of these compounds is shown in Figure 7.

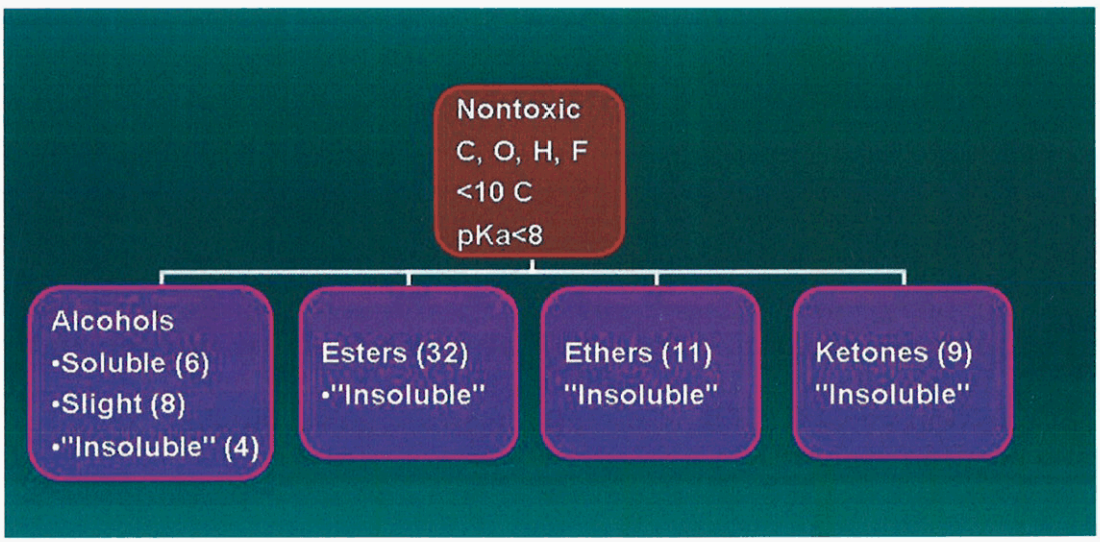

Figure 7. Results of the search for potential fluorinated tracers.

Three of the most soluble compounds were chosen for the initial screening tests that were conducted during FY 2001. These were conducted in our pressurized autoclaves at 280°C for four days. The compounds chosen were 3,3,3-trifluoro-1-propanol, 4,4,4- trifluorobutanol, and 1,1,1-

trifluoro-2-propanol. The screening tests indicated that he fluorinated alcohols were indeed more stable than their hydrocarbon analogues. It was decided to continue with the thermal stability tests during FY2002.

Results of the Fluorinated Alcohol Thermal Stability Tests

Experiments conducted during FY2002 defined the stability of the fluorinated alcohols in water at geothermal temperatures. Two of the compounds, 1,1,1-trifluoro-isopropanol and 4,4,4-trifluoro-n-butanol, were shown to be significantly more stable than their hydrocarbon analogues and the hydrofluorocarbon vapor-phase tracer R-134a (Figure 8). The third compound, 3,3,3-trifluoro-n-propanol proved to be similar in stability to both n-propanol and R-134a. This level of stability makes the fluorinated alcohols usable, but not spectacular, as geothermal tracers. For example, they are more stable than fluorescein (Adams and Davis, 1991) or R-134a (Adams and Kilbourn, 2000), and could be used at The Geysers or in a moderate-temperature liquid-dominated system. However, they are less stable than the naphthalene sulfonates (Rose et al., 2001) and could not be used in the multi-year tracer tests conducted with these polyaromatic sulfonates.

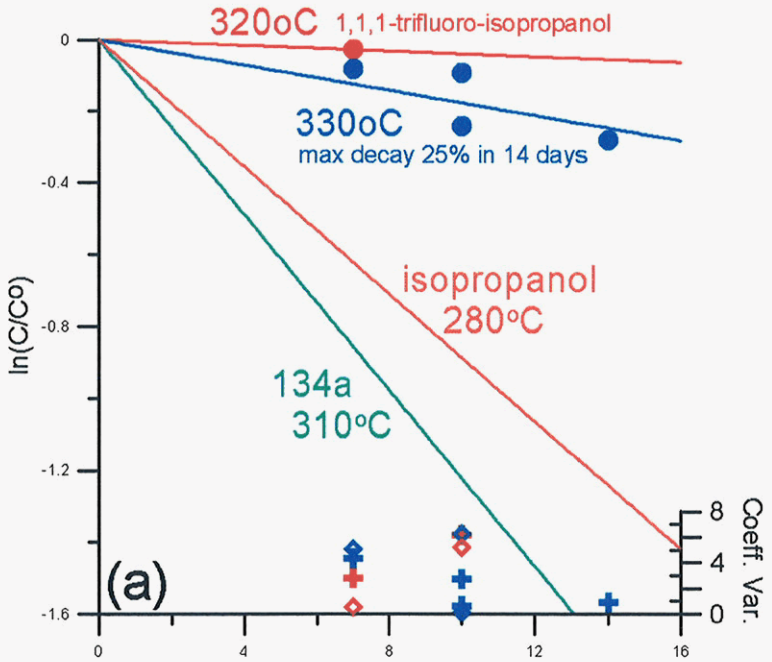

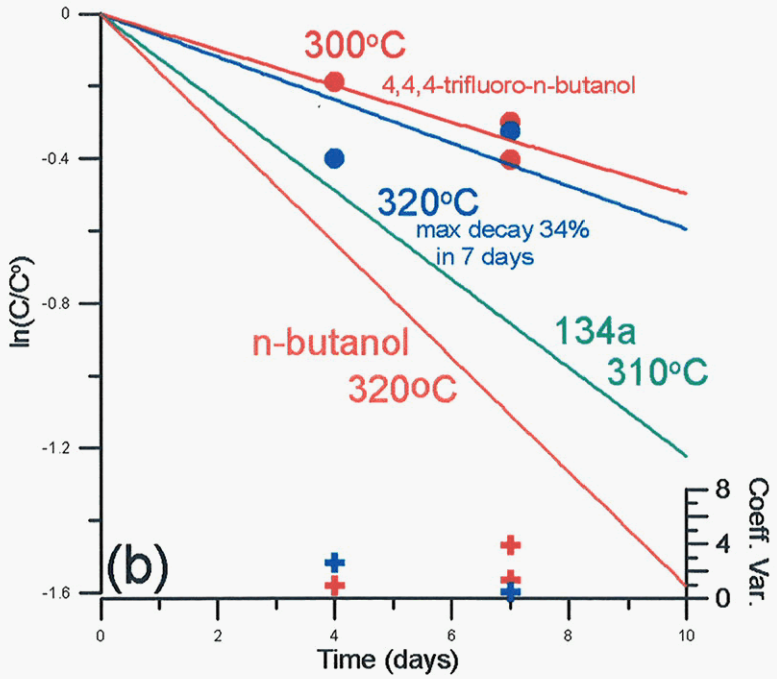

Figure 8. (a) Thermal stability of 1,1,1-trifluoro-isopropanol at 320° and 330°C. (b) Thermal stability of 4,4,4-trifluoro-n-butanol at 320° and 330°C. The stability of the hydrocarbon alcohol analogue and the hydrofluorocarbon vapor-phase tracer R-134a are shown for comparison. The coefficient of variation (stardard deviation/average; percent) of the sample preparation (diamonds) and analyses (crosses) of the fluorinated alcohols are shown at the bottom of each chart.

Estimation of Fluorinated Alcohol Detection Limits

Sensitive methods for detecting the vapor-phase tracers are generally developed by geothermal contractors. Such methods are not needed for the stability studies, but they are needed for field tests, which are performed by the contractors at The Geysers. A detection limit study was scheduled to be performed after the initial thermal stability studies. The study conducted by Thermochem, Inc, a company that is a standard supplier of chemical methods for the geothermal industry. This study was conducted to provide an indication of the detection limits that might be expected using conventional methods.

Their conclusions are as follows:

(1) The FID exhibited fairly high sensitivity for the fluorinated alcohol compounds tested, with detection limits below 200 ppb. However, the lack of selectivity may limit the application of this detector to actual geothermal fluid samples, which often contain a wide range of light hydrocarbons in ppb to ppm concentrations.

(2) The detection limit using the electrolytic conductivity detector (ELCD) by purge and trap could probably be extended into the 50 to 100 ppb range, assuming the contaminant can be eliminated, and larger sample volumes are purged. The signal to noise ratio of the ELCD will make it difficult to extend the detection limit any lower than this. The purge and trap method also yields a very low recovery for the fluorinated alcohol compounds due to their low volatility.

This study led to the decision made at the end of FY2002 that the fluorinated alcohols were not going to make good tracers. The factors involved in this decision were the poor detection limits, which were in contrast to our expectations for a fluorinated compound, the difficulty in handling the compounds and getting good kinetic data, their expense, and their possible transformation to toxic compounds in the reservoir. In FY2003 we set out to improve the detection limits for the hydrocarbon alcohols so that they could be used as two-phase tracers in the field.

Hydrocarbon Alcohol Detection Limits

Alcohols have been very infrequently used as geothermal tracers because they have a fairly high detection limit, and possess no special properties that make them strongly detectable. However, there is a new method for separating out polar hydrocarbons from water phase using SPME. Solid Phase Microextraction (SPME) is an innovative, solvent free technology that is fast, economical, and versatile. SPME is a fiber coated with a liquid (polymer), a solid (sorbent), or a combination of both. The fiber coating removes the compounds from the sample by absorption in the case of liquid coatings or adsorption in the case of solid coatings. The SPME fiber is then inserted directly into the Gas Chromatograph for desorption and analysis. SPME has gained wide spread acceptance as the technique of preference for many applications including flavors and fragrances, forensics and toxicology, environmental and biological matrices, and product testing to name a few. The variables involved in this method are the phase extracted, the temperature of the phase, the identity of the solid extraction phase, the time extracted, and the normal variables of the gas chromatograph. We have been exploring these variables and have succeeded in lowering the detection limit to the point where alcohols may be economic to use as tracers at The Geysers.

SPME extractions can be performed either by fiber immersion in the water solution or by exposure to the sample headspace. Immersion can be used when samples are "clean".

Headspace extractions can be optimized with heat, salinity, pH, and time. Increased water salinity reduces analyte solubility thereby increasing the concentration in the headspace. Heat drives more analyte into the headspace. Extraction efficiency increases with time until equilibrium between the fiber and the sample is reached. For the current evaluation sa-

linity and pH adjustments were not attempted. The key to quantification using SPME is keeping all analysis variables constant.

Preliminary results indicate that extraction times of 20 minutes in headspace at 40°C are sufficient to detect 10 ppb levels of n-propanol in water (Fig. 9). A temperature above 45°C is not recommended as it produces GC artifacts but no increased detection (Fig. 10). Our most recent efforts have reduced the n-propanol detection limits to 1 ppb (Fig. 11).

This work is encouraging as far as using alcohols as geothermal tracers is concerned, but more work still needs to be done on detection in a geothermal matrix and on the detectability of ethanol and methanol, which are more stable than propanol.

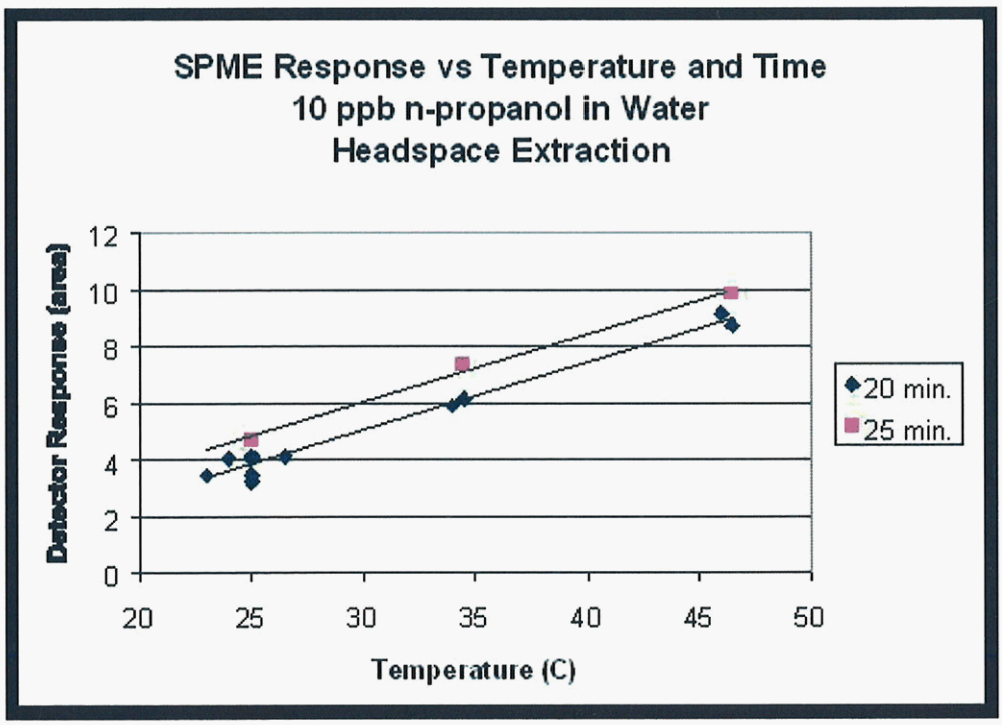

Figure 9. SPME response is a function of time and temperature. Detection limits are improved with increasing extraction time and at above room temperatures.

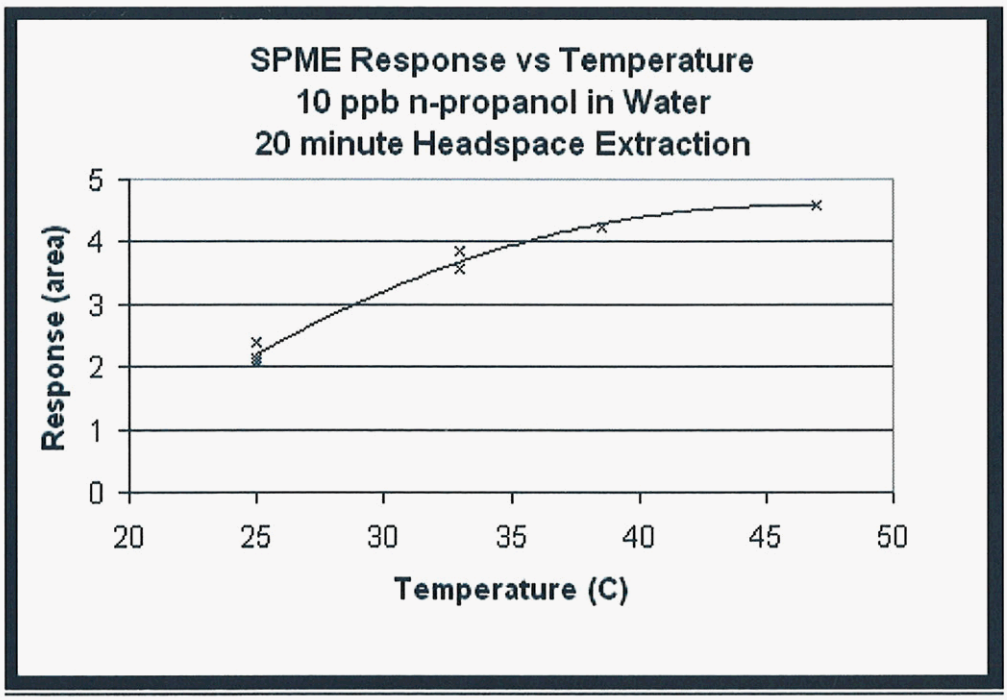

Figure 10. Temperature versus response curve showing that apparent optimum extraction temperature is between 40° and 50°C. It was observed that apparent GC anomalies were produced by water condensation at temperatures higher than 45°C.

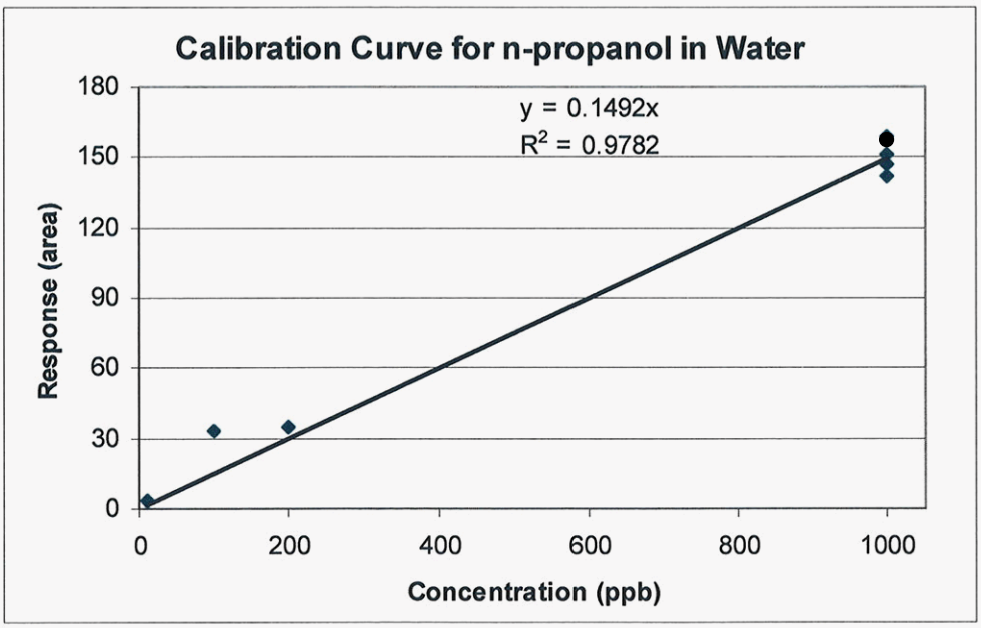

Figure 11. Calibration curve demonstrating that propanol can be used down to 1 part per billion.

Other Properties of Hydrocarbon Alcohols

Alcohols are essentially natural gases such as methane (one carbon), ethane (two carbons), propane (three carbons), and butane (four carbons) with a hydroxyl attached. The hydroxyl imparts a polar nature to the molecule and thus makes it soluble in water. The smaller alcohols such as methane, ethane, and propane are completely soluble in water, while butane and the heavier alcohols get less soluble in water as the molecular weight increases. The solubility of butane in water at room temperature is 7.1% by weight. Although alcohols contain an OH group, they have a pKa of greater than 14 at room temperature and should be neutral molecules under boiling conditions. The neutral charge allows them to fractionate easily to the steam phase.

The toxicity of alcohols varies. One measure is the TWA, which is the time-weighted average airborne concentration over an 8 hour working day, for a 5 day working week over an entire working life. These are 200, 1000, 200, and 150 ppm for methanol, ethanol, propanol, and butanol, respectively (ACGIH, 1979). Additional care should be taken with methanol because it can cause blindness at less-than-toxic concentrations.

These alcohols are relatively easy and inexpensive to purchase. Ethanol must either be denatured to prevent imbibition or a permit must be obtained for its purchase.

Liquid-Steam Distribution

The solubility of two-phase tracers such as the alcohols cannot be described by a simple temperature-dependent Henry's Law coefficient. This is because the same properties that produce solubility also modify the properties of the water as the concentration of the tracer increases. A more appropriate equation in this temperature range is the Wilson equation. This type of solubility predictor requires data sets in which concentration as well as temperature is varied. These data are used to produce optimized constants for the Wilson equation. Optimized parameters for methanol, ethanol, n-propanol, and n-butanol (the "n-" indicates no branching of the molecule) were taken from (GREEN, 1997), and were used to calculate the distribution coefficients (C_V/C_L) at various temperatures. Two caveats to these calculations are: 1) they are for alcohol-water binary systems, and 2) activity coefficient equations such as these are not dependable near or above the critical temperature of the solute, which for the alcohols are in the mid-200°C range. They are, however, sufficiently accurate to demonstrate that methanol will follow water very closely during boiling, with the other alcohols distributing more to the steam phase as the molecular weight increases (Fig. 12).

The discussion of solubility introduces another benefit of using the alcohols as tracers; they can be sampled as a liquid by quenching the steam in a cooling coil as it exits through the sample tubing. Figure 13 illustrates this point for n-propanol. At 10°C less than 20% of the tracer is in an equal volume of vapor at equilibrium with the liquid. If the sampling temperature is recorded the total amount of tracer can be back-calculated.

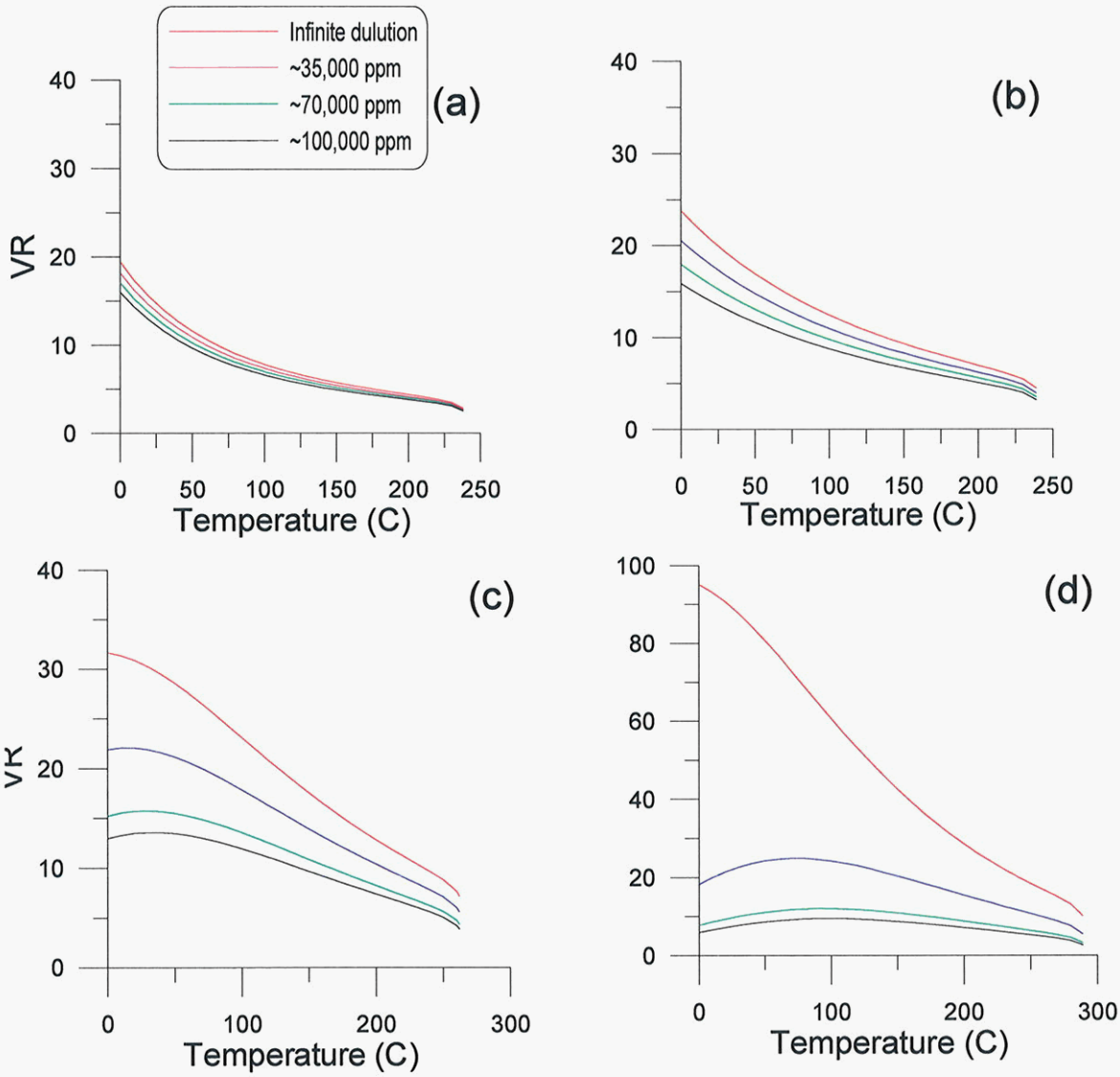

Figure 12. Distribution coefficients of (a) methanol, (b) ethanol, (c) n-propanol, and (d) n-butanol calculated using Wilson parameters taken from (GREEN, 1997).

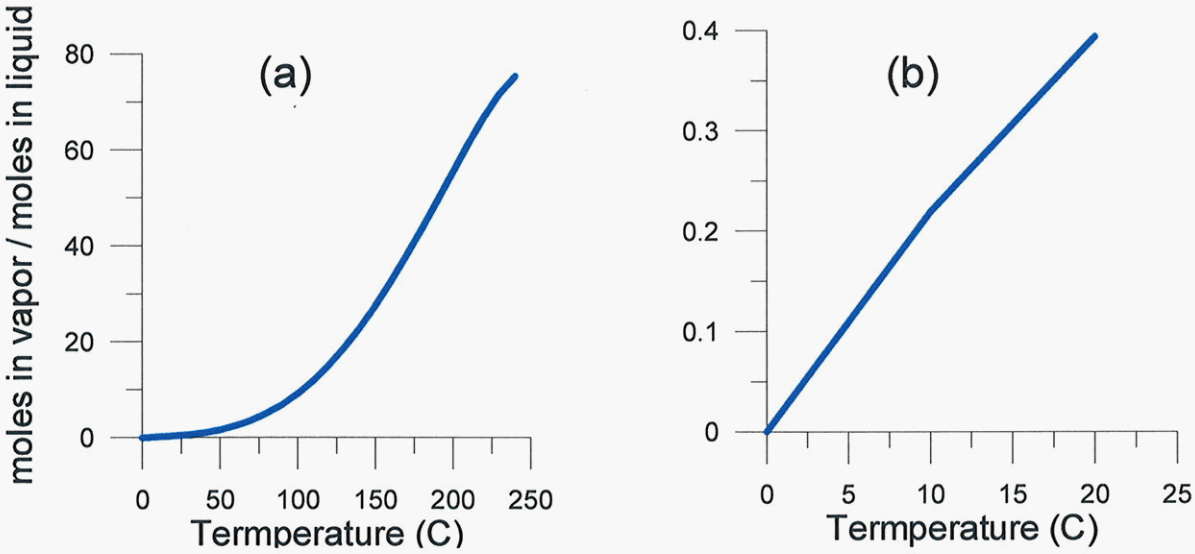

Figure 13. Distribution of propanol between an equal volume of liquid and vapor during sampling. The calculations demonstrate that quenching the steam limits the tracer lost to the vapor phase during sampling. (b) shows the low-temperature region of (a) in more detail.

Thermal Stability of the Alcohols

The data used in this analysis were selected from a larger pool of experimental results. Final concentrations in the experiments that are not included were, in general, substantially lower than those in similar experiments. It was concluded that this was the result of sporadic microbial action on the samples. Many of these experiments were performed within a specific time frame, so repeats were not always possible. The lack of repeats renders these results qualitative.

First-order kinetic rates were calculated from the rate data, and are displayed on an Arrhenius plot in Figure 14. This type of plot is based on the relationship:

$$\ln k = -E_a\left(\frac{1}{T}\right) + \ln A_O$$

where k is the rate constant, Ea is the activation energy, R is the Universal Gas Constant, T is the temperature in degrees Kelvin, and A_0 is the collision frequency factor. The minimum, maximum, and average of each temperature and pH condition are plotted. Salinity is not broken out because no significant difference was found between experiments that used 20 g/l NaCl solvents and those that used distilled water. The qualitative

nature of the data is obvious from the scatter of the points. However, the data are sufficient to make some generalizations and predictions.

Figure 14 shows that the order of stability is methanol (no decay, hence not on diagram) > ethanol > propanol > (propanol in acid solution) > butanol. This order is consistent with the observation that these compounds form a homologous series. A homologous series is a group of compounds with similar functional groups and a steadily varying but non-reactive carbon backbone. The activation energies calculated from the rates can be used to make rough predictions of the decay rates at other temperatures. These are shown for 200°, 250°, and 300°C in figure 15. In this figure the data scatter was incorporated as minimum and maximum rates, shown by the shaded area in the plots. It can be seen that any of the tracers could probably be used at 250°C, depending on the length of the test. The use of any but methanol could be problematic at temperatures above 300°C. However, methanol appears to be one of the decay products of ethanol, and propanol is among those produced from n-butanol. The byproduct identification was qualitative, so the absolute abundances of the byproducts are not known. If the lower-weight alcohols are significant products of the upper-weight alcohol, then they may be useful as reactive tracers.

Conclusions on Hydrocarbon Alcohols as Tracers

The alcohols methanol, ethanol, n-propanol, and n-butanol may be useful as geothermal tracers. Methanol is stable for long periods of time at temperatures over 300°C. Ethanol, n-propanol, and n-butanol are successively less stable, to the extent that butanol could only be used as a purely no-reactive tracer at temperatures less than 250°C. However, n-propanol has been reported as a decay product of butanol, as has methanol from ethanol decay, which opens the possibility of using them as reactive tracers. These alcohols are true two-phase tracers. Their liquid-vapor distribution coefficients at infinite dilution range from 6 to 42 at 150°C, which is far lower than the vapor-phase tracers, which have distribution coefficients in the thousands.

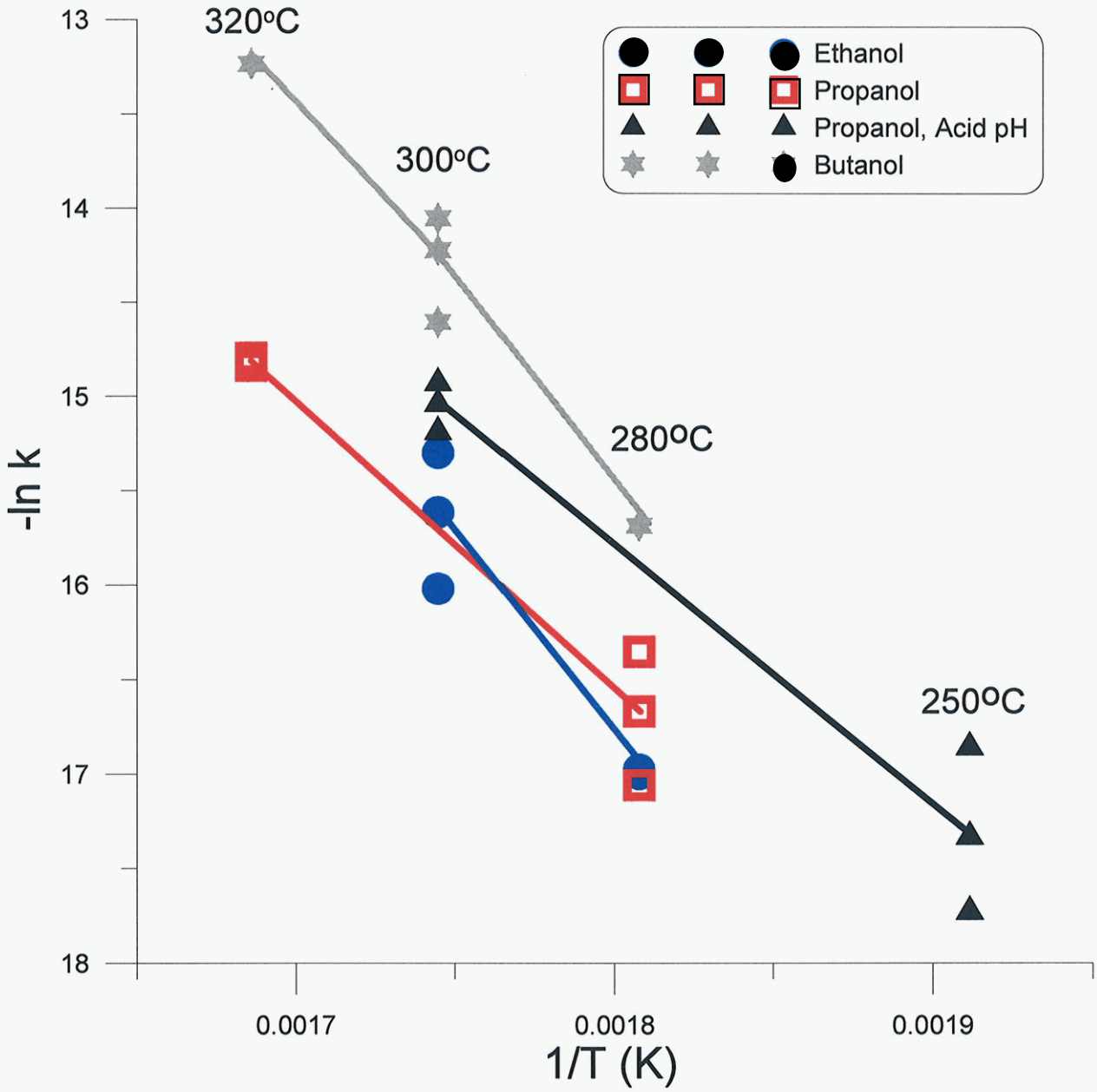

Figure 14. Arrhenius plot showing the relationship of the rate with inverse temperature. The minimum, average, and maximum rates are shown for each temperature.

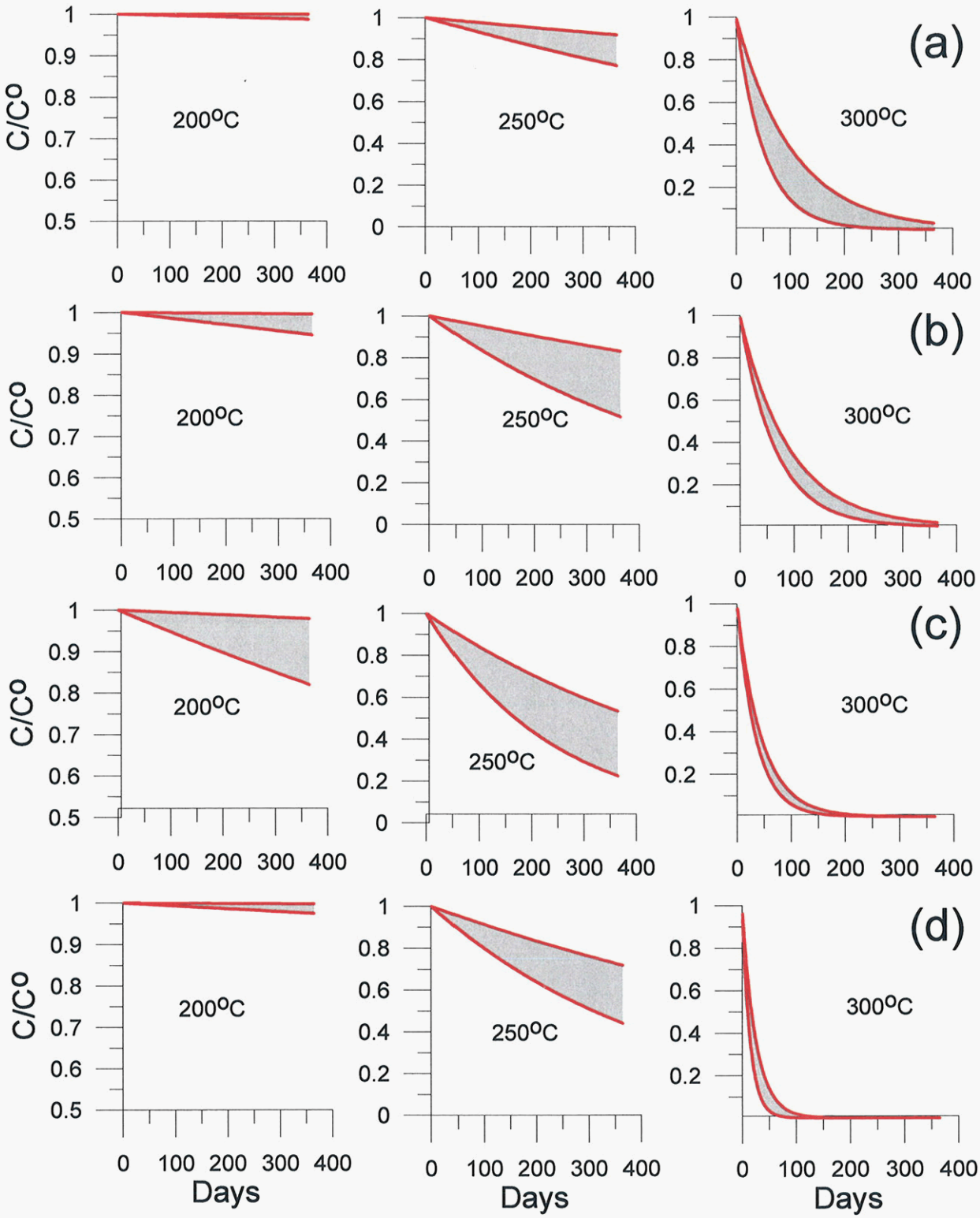

Figure 15. Estimated time-temperature decay curves for (a) ethanol, (b) propanol, (c) n-propanol in acid solution, (d) n-butanol.

Cove Fort Combined Tracer Test

We participated in a two-phase tracer test at the Cove Fort-Sulphurdale geothermal system. In this case a two-phase tracer was approximated by using both a liquid and a vapor-phase tracer. The Cove Fort-Sulphurdale geothermal system is located approximately 300 km south of Salt Lake City, within one of the largest thermal anomalies in the western U.S. (Fig. 16). The existence of this geothermal resource, which covers more than 47 km^2, was well known to the pioneers in the 1800's because of the presence of numerous fumaroles and altered alluvium containing native sulfur. Electricity is currently being produced from a shallow steam cap and the underlying liquid reservoir adjacent to a largest of the sulfur deposits (Fig. 16). The field and power plant, which are jointly owned by the Utah Municipal Power Agency (UMPA) and Provo City, generates 6-7 MWe from a combination of condensing and binary units. The plant came on line in 1985.

Figure 16 shows the locations of the production and injection wells. There are currently six production wells. Five of the wells discharge dry steam from fractured Mesozoic(?) sandstone that lies immediately below the Tertiary ash-flow tuffs. The depth to the top of the sandstone and the top of the steam cap decreases systematically from north to south. The deepest dry steam wells (Lady Olga, 34-7A; Lady Linda, 34-7B) produce steam from depths of 339-351 m. These wells had initial temperatures of 147°-151°C. P-89-1 (Lady Mary), located at the southern end of the field produces steam from 256-265 m. The sandstone appears to have a thickness of about 60 m.

P-91-4 produces water from the underlying liquid resource. This well was drilled to a depth of 745 m. P-94-1 is reported to have encountered steam at 258 m, the water table at 314 m, and a maximum temperature of 163°C. The water table appears to be located near the top of the limestones immediately below the sandstone. The limestones contain large open fractures or dissolution cavities. These were encountered at 542 m in P-94-1 and at 427 m in an adjacent deep slim hole. Below 600 m, P-94-1 encountered quartz monzonite. Liquid water is presently produced at a temperature of 152°C. After flashing through high and low pressure separators, the remaining water is injected into well 42-7 where it enters the reservoir at the base of the volcanic section between depths of 588 and 716 m. This water presently represents the sole source of injectate. Injection began in the middle of 1996. Well 42-7 was originally drilled to a depth of 2358 m and recorded a maximum temperature of 178°C near its base. To date, this is the highest temperature recorded in the field.

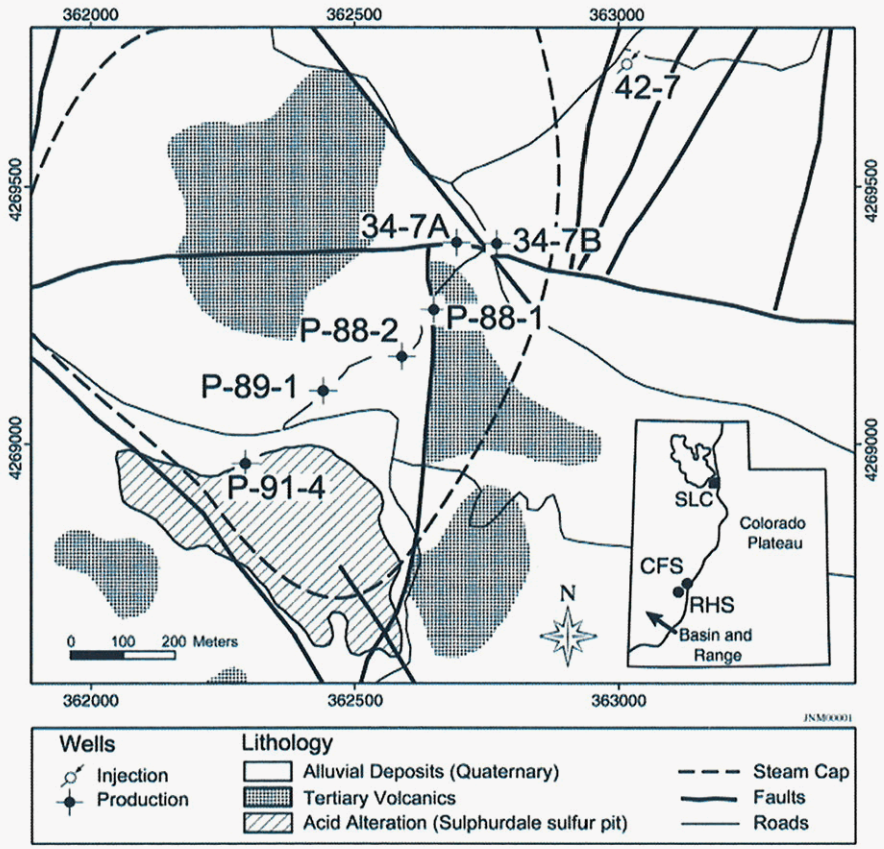

Figure 16. Geologic map of the Cove Fort-Sulfurdale geothermal system.

The full lateral and vertical extent of the vapor-dominated cap has not yet been defined by drilling. Self potential anomalies, low electrical resistivities, and the distribution of steam entries in the production wells suggest that it could underlie much of the western half of the area shown in Figure 16.

Tracer Test Description

Two hundred kilograms each of the liquid tracer fluorescein and the vapor-phase tracer R-134a were simultaneously injected into well 42-7 on January 14, 1999. Fluorescein was injected over a period of approximately 20 minutes. This was followed immediately by injection of R-134a over a four hour period.

The wells were sampled on the day of injection, then once per week for four months and then at progressively greater intervals as it became apparent that the tracer test would last for several years. The vapor-phase tracer was detected in the third round of sampling, two weeks after injection (Fig. 17). Within a month, all five wells were producing concentra-

tions of R-134a well above the detection limit of approximately 10 parts per trillion (ppt).

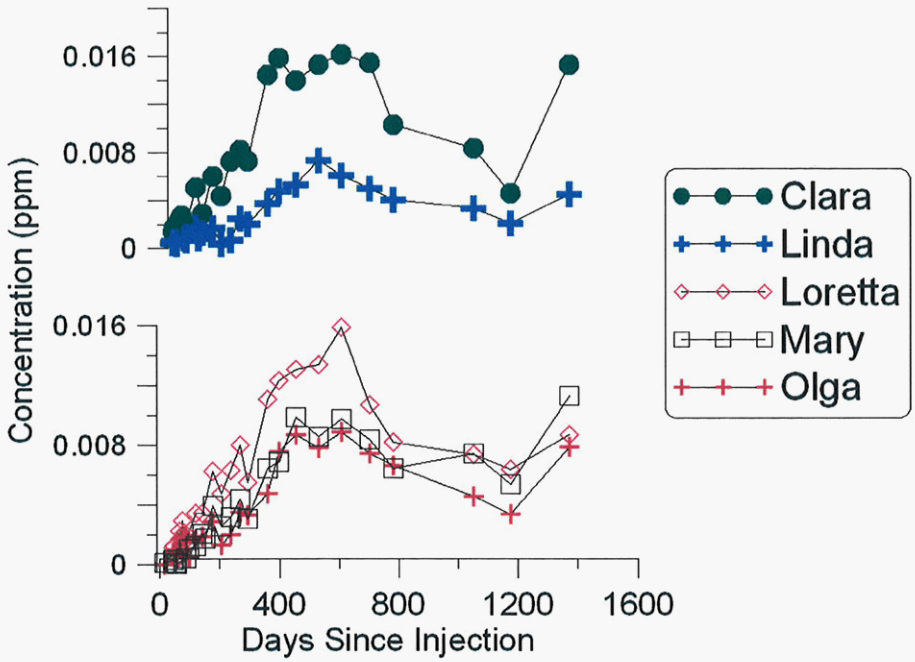

Figure 17. Tracer concentration versus time for R-134a at Cove Fort.

The concentrations of R-134a continued to rise, reaching peak values as high as 16 parts per billion (ppb) 1.6 years after injection. As of April, 2002, the concentrations of R-134a had returned to values as low as 2 ppb and were declining, so it was thought that tracer recovery was nearly over. However, concentrations in the most recent sample, taken in November, 2002, were nearly as high as the peak values.

This is probably the longest tracer test on record, certainly the longest vapor-phase tracer test. A vapor-phase tracer test generally lasts 50 days. The Cove Fort test is now approaching 1500 days. The shape of the tracer return curves suggests that the steam cap taps a small fraction of the injectate plume near the injection well, and that the majority of the tracer is still traveling slowly in the liquid phase. The most recent tracer increase may be a result of the tracer slug taking another fracture pathway and just now arriving at the steam reservoir. As shown in Figure 18, there is still a considerable fraction of the tracer still to be recovered.

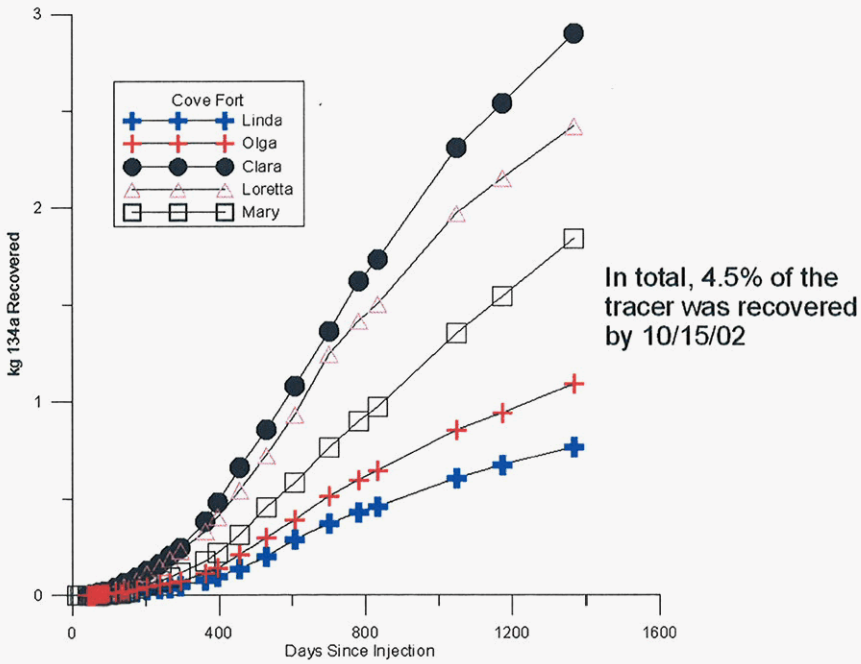

Figure 18. Cumulative recovery for each well in the Cove Fort geothermal system.

Task 4 – GIS Visualization and Data Processing

A suite of tools, automating several common calculations used in tracer interpretation, were created and reported by (NASH and ADAMS, 2001). These tools can be used to generate data in a format that is amenable for use in a GIS environment. However, changes in GIS technology, particularly the development and release of ArcGIS™ by ESRI recently, created a user and developer environment that allowed a much tighter integration of these tools as a custom user interface. This includes the automation of new toolbar generation and very simple installation and use. This is accomplished through accessing appropriate objects in ArcObjects™ and by creating new objects that are accessible to ArcMap™ using an object oriented programming language.

The new Tracer Toolkit (Figure 19) performs calculations on raw tracer data, automatically creates an ArcGIS compatible Shapefile with the results, and displays its contents as a point map (Figure 20). The user also has the option to define the coordinate system and datum of the map before it is generated. The map has topological links from the points to a database, which includes the calculated values by date, well names, and XY coordinates. The tools include (1) a utility to append tracer data and an XY coordinate file, (2) a raw data normalization function, (3) a log transform function for raw data, (4) an interpolation function, (5) a mass recovery function, and (6) a log transform function for interpolated data.

The point maps can then be used to generate statistical surfaces, contour maps, and 3-D renderings.

The input data must be in a comma delimited text format and XY coordinates must be included in two of the fields before the data fields begin. Tracer and steam flow data, in two separate files, are needed to calculate mass recovery.

The new tracer GIS interface is extremely easy to install and use. It is distributed as a single Dynamic Link Library (.dll) file. The user first places the .dll in a safe folder where it will not get deleted accidentally. The new toolbar is then placed into ArcMap by (1) going to the *Tools* pull-down menu and choosing *Customize* (Figure 21), (2) *Add From File* is then chosen and the TracersTools.dll is selected (Figure 22, (3) *Tracer Tools* is then checked under Toolbars, and (4) a new toolbar is then automatically created (Figure 23).

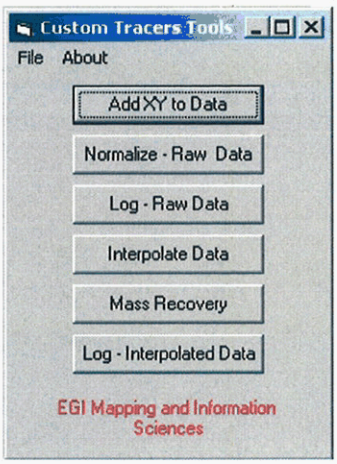

Figure 19. The new Tracer Toolkit interface.

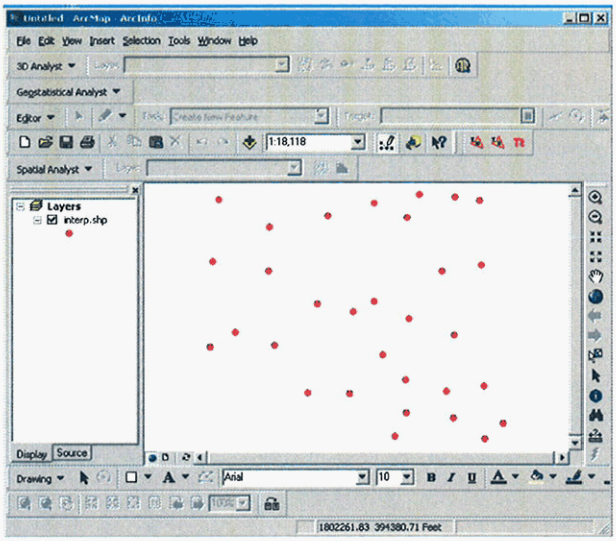

Figure 20. Point GIS map that is automatically produced from tracer data processed with the new Tracer Tool Kit.

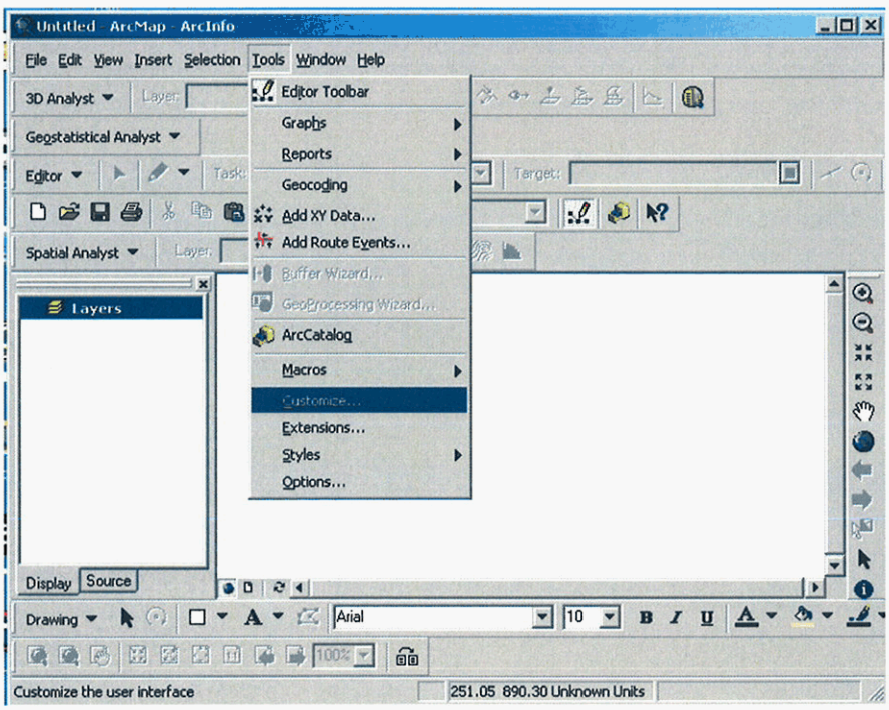

Figure 21. Installation of the new tracer tool kit is easily accomplished. The user first chooses Customize under the Tools pull-down menu.

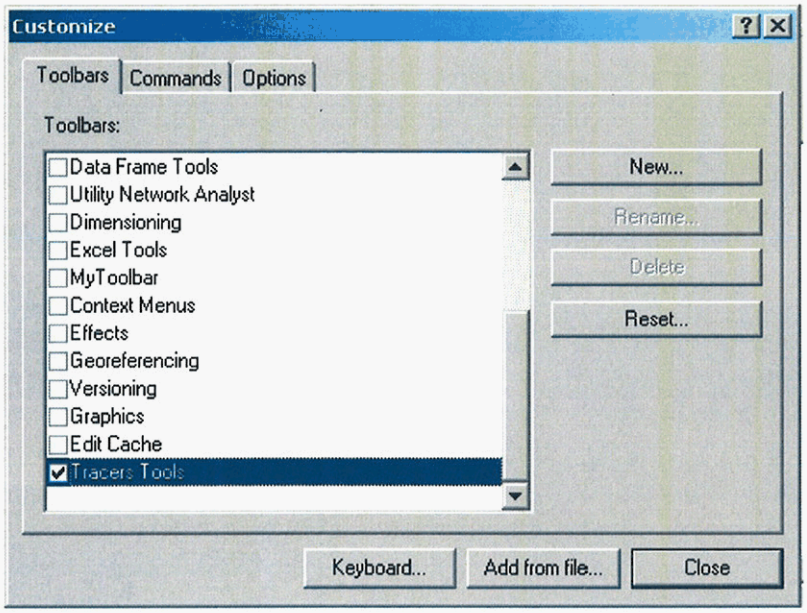

Figure 22. Add from file is then used to choose the TracersTools.dll file. Tracer Tools is then checked under Toolbars:

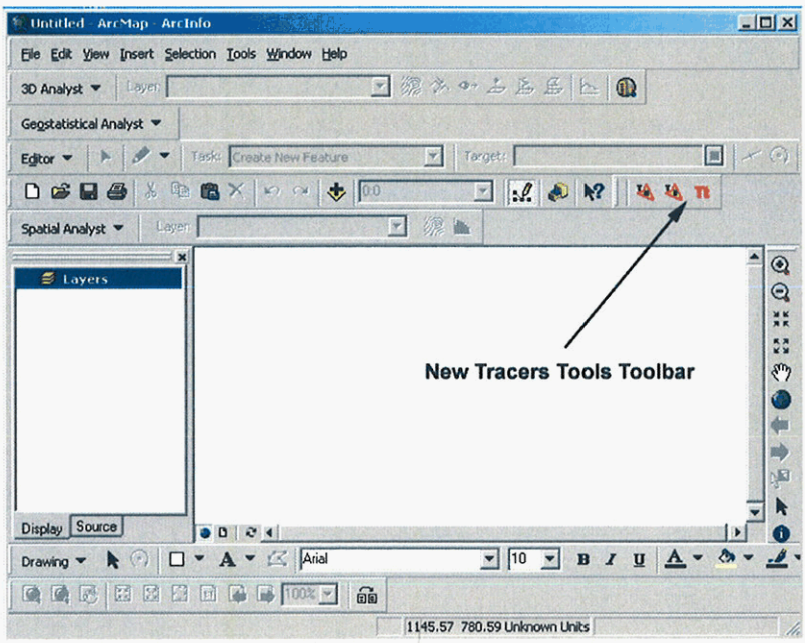

Figure 23. A new tool bar is automatically generated from which the toolkit interface, shown in Figure 19, is accessed.

Task 5 – Technology Transfer

Mike Adams gave two presentations on the use and properties of vapor-phase tracers at the Injection Technology short course given prior to the annual meeting of the Geothermal Resources Council in 1999 and 2000.

Papers for the special volume of Geothermics devoted to geothermal tracers, for which Mike Adams was guest editor, was published in FY 2002. The following papers were included:

Sullera, Ma. M., and Horne, R.N. Inferring injection returns from chloride monitoring data.

Shook, G. M. Predicting thermal breakthrough in heterogeneous media from tracer tests.

Axelsson, G., Flovenz, O. G., Hauksdottir, S., Hjartarson, A., and Liu, J. Results of tracer tests in the Laugaland geothermal field, N-Iceland, during 1997-1999.

Rose, P. E., Benoit, W. R., and Kilbourn, P. M. The application of the polyaromatic sulfonates as tracers in geothermal reservoirs.

Trew, M., and O'Sullivan, M. Modeling the phase partitioning behavior of gas tracers under geothermal reservoir conditions.

Lovelock, B.G. Steam flow measurement using alcohol tracers.

Hirtz, P., Kunzman, R., Broaddus, M., and Barbitta, J. Developments in Tracer Flow Testing for Geothermal Production Engineering.

Adams, M.C., Beall, J.J., Enedy, S.L., Hirtz, P.N., Kilbourn, P.M., Koenig, B.A., Kunzman, R., and Smith, J.L.B. Hydrofluorocarbons as Geothermal Vapor-Phase Tracers.

Publications

Thirteen papers were published under this contract in addition to the Tracer Special Volume. These are:

Adams M. C. (2001) A comparison of two multiple-tracer tests conducted at The Geysers. *Twenty-Sixth Workshop on Geothermal Reservoir Engineering.*

Adams M. C. (2003) Use of the Chloride to Boron Ratio in Monitoring Two-Phase Conditions in the Coso Reservoir. *2003 Coso Research Symposium.*

Adams M. C. (2004) Use of Naturally-Occurring Tracers to Monitor Two-Phase Conditions in the Coso Reservoir. *Twenty-Ninth Workshop on Geothermal Reservoir Engineering.*

Adams M. C., Beall J. J., Enedy S. L., Hirtz P. N., Kilbourn P., Koenig B. A., Kunzman R., and Smith J. L. B. (2001) Hydrofluorocarbons as geothermal vapor-phase tracers. *Geothermics* **30**, 747-775.

Adams M. C., Beall J. J., Hirtz P., Koenig B. A., and Smith J. L. B. (1999) Tracing effluent injection into the SE Geysers - a progress report. *Transactions, Geothermal Resources Council*, 341-345.

Adams M. C. and Kilbourn P. M. (2000) Thermal stability of the vapor-phase tracer R-134a. *Twenty-Fifth Workshop on Geothermal Reservoir Engineering.*

Adams M. C., Moore J. N., Bjornstad S., and Norman D. I. (2000a) Geologic history of the Coso geothermal system. *World Geothermal Congress*, 2463-2469.

Adams M. C., Yamada Y., Yagi M., Kasteler C., Kilbourn P., and Dahdah N. (2004) Alcohols as tracers. *Twenty-Ninth Workshop on Geothermal Reservoir Engineering.*

Adams M. C., Yamada Y., Yagi M., Kondo T., and Wada T. (2000b) Stability of methanol, propanol, and SF6 as high-temperature tracers. *World Geothermal Congress*, 3015-3019.

Beall J. J., Adams M. C., and Hirtz P. N. (1998) Evaluation of R-134a as an injection tracer in the Southeast Geysers. *Transactions, Geothermal Resources Council*, 569-573.

Beall J. J., Adams M. C., and Smith J. L. B. (2001) Geysers reservoir dry out and partial resaturation evidenced by twenty-five years of tracer tests. *Transactions, Geothermal Resources Council*, in press.

Bloomfield K. K., Moore J. N., Adams M. C., and Sperry T. L. (2001) Tracer test design and sensitivity studies of the Cove Fort geothermal resource tracer test. *Transactions, Geothermal Resource Council.*

Moore J. N., Adams M. C., Sperry T. L., Bloomfield K. K., and Kunzman R. (2000) Preliminary results of geochemical monitoring and tracer tests at the Cove Fort-Sulphurdale geothermal system, Utah. *Twenty-Fifth Workshop on Geothermal Reservoir Engineering.*

Nash G. D. and Adams M. C. (2001) Cost effective use of GIS for tracer test data mapping and visualization. *Transactions, Geothermal Resources Council*, in press.

Acknowledgements

This material is based upon work supported by the U. S. Department of Energy under Award No. DE-FG07-00ID13893. Any opinions, findings, and conclusions or recommendations expressed in this material are

those of the authors and do not necessarily reflect the views of the Department of Energy.

References

ACGIH. (1979) *TLV's - Threshold limit values for chemical substances and physical agents in the workroom environment.* American Conference of Governmental Industrial Hygenists.

Adams M. C. (1985) Tracer stability and chemical changes in an injected geothermal fluid during injection-backflow testing at the East Mesa geothermal field. *Tenth Workshop on Geothermal Reservoir Engineering*, 247-252.

Adams M. C. (1997) New tracers take on The Geysers. *Geothermal Technologies* **2** 1-2.

Adams M. C. (1999) Tracing the flow of effluent into The Geysers geothermal field. In *Research Summaries, FY98.* U. S. Department of Energy, Office of Geothermal Technologies.

Adams M. C. (2001) A comparison of two multiple-tracer tests conducted at The Geysers. *Twenty-Sixth Workshop on Geothermal Reservoir Engineering.*

Adams M. C., Beall J. J., Enedy S. L., and Hirtz P. (1991a) The application of halogenated alkanes as vapor-phase tracers: A field test in the Southeast Geysers. *Transactions, Geothermal Resources Council*, 457-463.

Adams M. C., Beall J. J., Enedy S. L., Hirtz P. N., Kilbourn P., Koenig B. A., Kunzman R., and Smith J. L. B. (2001) Hydrofluorocarbons as geothermal vapor-phase tracers. *Geothermics* **30**, 747-775.

Adams M. C., Beall J. J., Hirtz P., Koenig B. A., and Smith J. L. B. (1999) Tracing effluent injection into the SE Geysers - a progress report. *Transactions, Geothermal Resources Council*, 341-345.

Adams M. C., Benoit W. R., Doughty C., Bodvarsson G. S., and Moore J. N. (1989) The Dixie Valley, Nevada tracer test. *Transactions, Geothermal Resources Council*, 215-220.

Adams M. C. and Davis J. (1991) Kinetics of fluorescein decay and its application as a geothermal tracer. *Geothermics* **20**, 53-66.

Adams M. C. and Kilbourn P. M. (2000) Thermal stability of the vapor-phase tracer R-134a. *Twenty-Fifth Workshop on Geothermal Reservoir Engineering.*

Adams M. C., Moore J. M., and Hirtz P. (1991b) Preliminary assessment of halogenated alkanes as vapor-phase tracers. *Sixteenth Workshop on Geothermal Reservoir Engineering*, 57-62.

Adams M. C., Moore J. N., Fabry L., and Ahn A. H. (1992) Thermal stabilities of aromatic acids as geothermal tracers. *Geothermics* **21**, 323-339.

Beall J. J., Adams M. C., and Hirtz P. N. (1994) R-13 tracing of injection in The Geysers. *Transactions, Geothermal Resources Council*, 151-159.

Beall J. J., Adams M. C., and Hirtz P. N. (1998) Evaluation of R-134a as an injection tracer in the Southeast Geysers. *Transactions, Geothermal Resources Council*, 569-573.

Bixley G., Glover R. B., McCabe W. J., Barry B. J., and Jordan J. T. (1995) Tracer calibration tests at the Wairakei geothermal field. *World Geothermal Congress*, 1887-1891.

Drummond S. E., Jr. (1981) Boiling and mixing of hydrothermal fluids: chemical effects on mineral precipitation. Ph.D., Pennsylvania State University.

Green D. W. (1997) Perry's Chemical Engineer's Handbook. McGraw-Hill.

Gudmundsson J. S., Hauksson T., Thorhallsson S., Albertson A., and Thorolfsson G. (1984) Injection and tracer testing in Svartsengi Field, Iceland. *Proceedings of the Sixth New Zealand Geothermal Workshop*, 175-180.

Gudmundsson J. S., Johnson S. E., Horne R. N., Jackson P. B., and Culver G. G. (1983) Doublet tracer testing in Klamath Falls, Oregon. *Ninth Workshop on Geothermal Reservoir Engineering*, 331-337.

Henley R. W. (1984) Gaseous components in geothermal processes. In *Fluid Mineral Equilibria in Hydrothermal Systems*, Vol. 1, pp. 45-54. The Economic Geology Publishing Company.

Horne R. N., Johns R. A., Adams M. C., Moore J. N., and Stiger S. G. (1987) The use of tracers to analyze the effects of reinjection into fractured geothermal reservoirs. *Geothermal Program Review V*, 37-52.

McCabe W. J., Barry B. J., and Manning M. R. (1983) Radioactive tracers in geothermal underground water flow studies. *Geothermics* **12**, 83-110.

Moore J. N., Adams M. C., Sperry T. L., Bloomfield K. K., and Kunzman R. (2000) Preliminary results of geochemical monitoring and tracer tests at the Cove Fort-Sulphurdale geothermal system, Utah. *Twenty-Fifth Workshop on Geothermal Reservoir Engineering.*

Nash G. D. and Adams M. C. (2001) Cost effective use of GIS for tracer test data mapping and visualization. *Transactions, Geothermal Resources Council*, in press.

Rose P. E. and Adams M. C. (1994) The application of rhodamine WT as a geothermal tracer. *Transactions, Geothermal Resources Council*, 237-240.

Rose P. E., Benoit W. R., and Kilbourn P. (2001) The application of the Polyaromatic sulfonates as tracers in geothermal reservoirs. *Geothermics* **30**(6), 617-640.

Upstill-Goddard R. C. and Wilkins C. S. (1995) The potential of SF6 as a geothermal tracer. *Water Research* **29**, 1065-1068.

Voge E., Koenig B., Smith J. L., Enedy S., Beall J. J., Adams M. C., and Haizlip J. (1994) Initial findings of The Geysers Unit 18 cooperative injection project. *Transactions, Geothermal Resources Council*, 353-357.